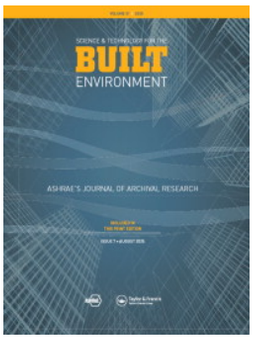

Science and Technology for the Built Environment

ISSN: 2374-4731 (Print) 2374-474X (Online) Journal homepage: www.tandfonline.com/journals/uhvc21

Parametric analysis of a three-stage cascade refrigeration system for ultra-low temperature applications and performance prediction using multilayer perceptron algorithm

Oguzhan Pektezel

To cite this article: Oguzhan Pektezel (2025) Parametric analysis of a three-stage cascade refrigeration system for ultra-low temperature applications and performance prediction using multilayer perceptron algorithm, Science and Technology for the Built Environment, 31:7, 723-747, DOI: 10.1080/23744731.2025.2523204

To link to this article: https://doi.org/10.1080/23744731.2025.2523204

Science and Technology for the Built Environment, (2025) **31**, 723–747

ISSN: 2374-4731 print / 2374-474X online
DOI: 10.1080/23744731.2025.2523204

Taylor & Francis
Taylor & Francis Group

Parametric analysis of a three-stage cascade refrigeration system for ultra-low temperature applications and performance prediction using multilayer perceptron algorithm

OGUZHAN PEKTEZEL*

Department of Mechanical Engineering, University of Balikesir, 10145 Balikesir, Turkey

In this study, the thermal design of a three-stage cascade refrigeration system capable of operating at ultra-low temperatures was conducted. In the first part of the study, a parametric performance analysis was performed using six refrigerant groups: R1150/R170/R717, R1150/R170/R1270, R1150/R170/R1234yf, R1150/R744/R717, R1150/R744/R1270, and R1150/R744/R1234yf. The results showed that the most efficient refrigerant group was R1150/R170/R717, and with this group, a COP of 0.65 and an exergy efficiency of 0.35 were achieved at an evaporator temperature of −85 °C. In the second part of the study, a dataset was created using the most efficient operating parameters identified from the parametric analysis, and a prediction study was conducted using the MLP algorithm. It is important to note that, for the first time in the literature, machine learning was applied to a three-stage cascade refrigeration system. The findings revealed MAE values of 0.0006, 0.0193, 0.0003, and 0.0194 for COP, total compressor power consumption, exergy efficiency, and total exergy destruction predictions, respectively, in the test set. It is important to highlight that the thermodynamic and artificial intelligence analyses performed for the three-stage cascade refrigeration system in this study will serve as a model for ultra-low temperature refrigeration system designs.

1. Introduction

The emergence of the SARS-CoV-2 vaccines as a result of COVID-19 declared as a global pandemic by World Health Organization in March 2020 has highlighted a long-standing issue in society: deep freezing and ultra-low temperature refrigeration. Pfizer-BioNTech disclosed that their vaccines must be stored at temperatures ranging from −60 °C to −80 °C (Udroiu, Mota-Babiloni, and Navarro-Esbrí 2022). Therefore, the development of refrigeration systems that can keep vaccines at this low temperature has become increasingly important. It was declared by Indian Ministry of Health that over 50% of vaccines in India fail annually due to the inability to maintain proper storage temperatures during transportation and distribution, leading to significant financial losses and resource wastage (Ji et al. 2024). Multi-stage compression and cascade refrigeration systems (CRS) have been put forward as viable solutions for these applications (Ye et al. 2024a). The same refrigerant circulates in multi-stage vapor compression refrigeration systems while different refrigerant couples are used in cascade refrigeration systems.

Recently, the utilization of ultra-low temperature freezing has gained widespread adoption, particularly in fields such as hypothermal medicine, liquefied gases, electronic communication, and food preservation (Ye et al. 2024b). Single-stage vapor compression refrigeration system is inadequate for achieving low temperatures. This is due to the high pressure ratio, high discharge pressure, and oil temperature, which lead to reduced volumetric efficiency and a lower coefficient of performance (COP) for the system (Rezayan and Behbahaninia 2011). One of the differences between CRS and conventional refrigeration systems is that, for a given cooling capacity, although the COP of CRS is slightly lower, it can achieve lower temperatures. Consequently, cascade refrigeration systems composed of multiple vapor compression cycles have been proposed to achieve the desired low refrigeration temperatures. Temperatures below −50 °C can be classified as ultra-low temperature refrigeration according to the American Society of Heating, Refrigerating, and Air-Conditioning Engineers (ASHRAE) (Mota-Babiloni et al. 2020). Scientific experiments conducted in low-temperature conditions, organ preservation, and the storing of specialized food products (such as rapid freezing of ice cream and tuna preservation) necessitate temperatures below −50 °C (Chen et al. 2023).

Received April 1, 2025; accepted June 5, 2025
Oguzhan Pektezel, BSc, MSc, PhD, is an Assistant Professor.

*Corresponding author e-mail: oguzhan.pektezel@balikesir.edu.tr

Refrigeration systems exhibit high energy consumption due to compressor operation and contribute to the greenhouse effect (Pektezel, Das, and Acar 2023a). It is well established that refrigeration applications account for a substantial portion of global energy consumption, with estimates indicating that approximately 17% of the world's total energy usage is attributed to refrigeration systems (Pektezel, Das, and Acar 2023b). International Institute of Refrigeration estimates that the electricity consumption caused by the refrigeration applications will be doubled or even tripled when it comes to 2050 (Hamzaoui, Tiachacht, and Hadiouche 2024b). Cascade systems offer significant energy-saving potential not only for refrigeration applications but also for heat pump systems (Ustaoglu et al. 2020).

In recent years, the performance enhancement of cascade refrigeration systems and the selection of suitable refrigerants have attracted significant attention from researchers. Majority of the studies carried out in cascade refrigeration systems are two-stage applications. In a study conducted by Ye et al. (2024b), researchers applied ANN together with parametric analysis in a two-stage cascade refrigeration system using R170 and R290 refrigerants. Evaporator and condenser temperatures were designed as −95 °C and 35 °C, respectively. The results revealed that the condensing temperature of the low-temperature cycle has an optimum value, which maximizes the COP and exergy efficiency, thus minimizing the total compressor consumption and exergy destruction. In addition, ANN artificial intelligence findings resulted in MAE values of 0.0027, 0.9090, 1.0314 and 0.1691 for COP, compressor consumption, exergy destruction, and exergy efficiency, respectively. Sun et al. (2016) analyzed the thermodynamic performance of R41/R404A and R23/R404A refrigerant pairs in a two-stage cascade refrigeration cycle. In the analysis, the evaporator temperature varied between −60 °C and −30 °C. The results showed that the maximum exergy efficiency was 44.38% for R41/R404A and 42.98% for R23/R404A. Faruque, Uddin, et al. (2022) analyzed the performance of various hydrocarbon class refrigerants in a two-stage cascade refrigeration system where the evaporator and condenser temperatures were −40 °C and 40 °C, respectively. For this purpose, they used Trans-2-butane in the low temperature cycle and Toluene, Cyclopentane and Cis-2-butane in the high temperature cycle. It was detected that when the condenser temperature of low temperature circuit changed from −25 °C to 30 °C, Trans-2-butane/Toluene refrigerant pair exhibited the best performance, with the greatest COP value of 1.96, lowest compressor consumption of 6.27 kW, the biggest exergy efficiency of 55.7% and the lowest exergy destruction value of 2.84 kW. Ye et al. (2024a) applied the response surface methodology in a two-stage refrigeration cycle using R170/R290 refrigerant pair. The results showed that the optimum evaporator and condenser temperatures were −97.87 °C and 30.39 °C and the optimum COP and exergy efficiency under these conditions were 0.6% and 40.73%. Chen et al. (2023) investigated the effect of using an internal exchanger on performance of a two-stage cascade refrigeration system where the evaporator temperature varied between −80 °C and −50 °C and the cooling capacity was 9 kW. They compared the conventional R23/R404A pair by using ammonia in the high temperature cycle and R1150, R170 and R41 in the low temperature cycle. It was declared that when mounting an internal heat exchanger to the system, COP of the R1150, R170 and R41 systems decreased by 8.03%, 6.99% and 12.68% in comparison with the system not using an internal heat exchanger. However, the use of an internal heat exchanger for R23/R404A system increases COP by 12.63% compared to conventional cycle. It was also determined that when the evaporator temperature was −60 °C and the condenser temperature was 40 °C, the COP of R1150/Ammonia, R170/Ammonia and R41/Ammonia systems increased by 9.87%, 13.39% and 13.51% in comparison with R23/R404A system, respectively. Sun et al. (2019b) carried out performance analysis with different combinations of refrigerants in a two-stage cascade refrigeration system where the evaporator temperature varied between −85 °C and −30 °C and the cooling capacity was 10 kW. R290, R717, R1270, R161, R32, R1234yf and R1234ze working fluids were utilized in the high-temperature cycle and R23, R41 and R170 fluids were used in the low-temperature cycle. The results showed that at temperatures lower than −60 °C, the COP value and thermodynamic performance of the R170/R161 pair were superior to the other refrigerants used, while at temperatures higher than −60 °C, the efficiency of the R41/R161 pair was higher than the other fluids. When the evaporator temperature increased from −85 °C to −30 °C, the COP for R170/R161 increased from 0.7 to 2.06 and for R41/R161 from 0.66 to 2.10. Ji et al. (2024) analyzed the performance of eight different refrigerant pairs, namely R404A-R508B, R1234yf-R170, R1234yf-R1150, R717-R170, R717-R1150, R290-R170, R290-R1150 and R1270-R170 in a two-stage cascade refrigeration cycle. In the analysis, evaporator temperature changed from −85 °C to −65 °C, condenser temperature varied between 30 °C and 50 °C, and the cooling capacity was 5 kW. The analysis result revealed that R290-R170 pair was the optimum refrigerant pair and caused an increase in COP by 5.94% and a decrease in compressor power consumption by 5.68% compared to R404A-R508B pair.

There have been a limited number of studies about three-stage cascade refrigeration systems. Hamzaoui, Hadiouche, and Tiachacht (2024a) analyzed the performance of R1150/R170/R717, R1150/R170/R290, R1150/R170/R1270, and R1150/R170/RE170 refrigerants in a three-stage cascade refrigeration system. The performance analysis revealed that the COP is inversely proportional to the condensation temperature and directly proportional to the evaporation temperature, with COP values ranging from 0.35 to 0.9. The results indicated that the R1150/R170/RE170 refrigerant group demonstrated the best energy, exergy, and environmental performance. Additionally, it was noted that increasing the temperature difference between the condensation and evaporation stages affects the compressor discharge temperature, potentially exceeding 125 °C for R717, which may lead to lubrication issues. Rogala and Kwiatkowski (2022) investigated the potential of a three-stage cascade refrigeration system to operate in the range of 110 K to 150 K. They designed two different system configurations: in the first

design, single-stage compression was applied at each stage, while in the second design, two-stage compression was applied at the second and third stages. The evaluation of the designs indicated that temperatures below 130 K could only be achieved with two-stage compression and the use of R50. The results showed that the lowest temperature reached in the three-stage cascade refrigeration system was 127 K, with a COP value of 0.179 Sun and Wang (2022) configured the conventional two-stage cascade refrigeration system by placing two compressors in both the LTC and HTC cycles, enabling two-stage compression in each cycle. They compared the obtained results with a conventional three-stage cascade refrigeration system. The results showed that the proposed new system reduced compressor power consumption by 1.4–1.7 kW and increased the COP value by 7%–11.7% compared to the conventional three-stage cascade system. Hamzaoui, Tiachacht, and Hadiouche (2024b) conducted a performance study on a three-stage cascade refrigeration system using R50/R1150/R290 and R50/R1150/R1270 refrigerants. Evaporator temperatures ranging from −160 °C to −120 °C, condenser temperatures ranging from 30 °C to 55 °C, and 10 kW of cooling capacity were selected as operating parameters. It was detected that R290 showed better performance than R1270. It was also stated that an increase in condenser temperature caused exergy efficiency to firstly increase and then decrease, while increase in evaporator temperature caused an increase in exergy efficiency. Walid Faruque, Uddin, et al. (2022) performed thermodynamic analysis using hydrocarbon refrigerants in a triple cascade refrigeration system. Four different refrigerant groups were used in the analysis: 1-butene/Heptane/m-Xylene, 1-butene/Trans-2-butene/m-Xylene, 1-butene/Toluene/m-Xylene and 1-butene/Cis-2-butene/m-Xylene. In addition, the evaporator temperature was changed between −120 and −90, while the cooling load was selected as 10 kW. It was determined that 1-butene/Heptane/m-Xylene group caused the biggest system performance at −120 °C and −110 °C evaporator temperatures, while 1-butene/Toluene/m-Xylene group gave the highest performance at evaporator temperatures of −100 °C and −90 °C. In addition, the maximum COP and exergy efficiency values at −100 °C evaporator temperature were detected to be 0.5931 and 54.446%, respectively. Kayes et al. (2024) performed thermodynamic analysis on a triple cascade refrigeration system operating with 1-butene/Heptane/m-Xylene refrigerant group. They used evaporator temperatures ranging from −140 °C to −101 °C and condenser temperatures ranging from 36 °C to 60 °C as design parameters, and the cooling capacity was determined as 10 kW. The optimum operating conditions were determined as −101 °C evaporator and 36.5 °C condenser temperatures. It was revealed that the COP and exergy efficiency realized under optimum conditions were 0.71 and 0.51, respectively. It was also found that increasing the evaporator temperature from −140 °C to −104 °C caused a 91.2% increase in COP and 83.7% increase in exergy efficiency. Additionally, it was detected that with the increase of condenser temperature from 36 °C to 58 °C, COP and exergy efficiency decreased by 15.7% and 16.2%, respectively. In a study carried out by Sun et al. (2019a), researchers performed performance analysis using different combinations of R1150 in the low temperature cycle, R41 and R170 in the medium temperature cycle, and R290, R161, R717, R1234yf, R1234ze, R1270, R152a and R32 in the high temperature cycle in a three-stage refrigeration system. In the analysis, the evaporator temperature was changed between −120 °C and −80 °C, the condenser temperature was assumed as 40 °C, and the cooling capacity was assumed as 10 kW. It was found out that utilizing R161 and R152a as high temperature cycle refrigerants resulted in the biggest COP while using R1234yf caused the lowest. In addition, it was declared that R170 as medium temperature cycle refrigerant was found to be more efficient in terms of COP compared to R41. Nabil et al. (2023) proposed an improved triple cascade refrigeration system configuration by adding a flash tank and a suction line heat exchanger. They used m-Xylene, Toluene, and 1-Butene group as refrigerants in the system. It was shown that the proposed system caused a 19.33% decrease in compressor consumption and a 22% increase in COP. It was also determined that the exergy efficiency increased by 19.35% compared to traditional triple cascade refrigeration systems with the proposed system, and it was reported that 49.015% exergy efficiency was achieved with this system.

The most widely utilized cascade refrigeration systems are typically two-stage cycles. Nevertheless, their performance declines significantly when achieving extremely low temperatures, necessitating the implementation of three-stage cascade refrigeration systems. Three-stage cascade refrigeration systems are employed in industrial refrigeration applications, effectively meeting the cooling demands for temperatures below −80 °C. It is noteworthy that research on three-stage cascade refrigeration systems remains relatively scarce. In addition, artificial intelligence application in there-stage cascade refrigeration systems has not been encountered in the literature review. In the literature, studies on the application of artificial intelligence to thermal systems have been gaining momentum. Moreover, numerous studies have been conducted on the application of machine learning methods in various experimental refrigeration systems or theoretical refrigeration system designs. In this context, applying machine learning methods to three-stage cascade refrigeration systems—a relatively new configuration with limited detailed analyses—could be highly beneficial when these systems move to the experimental setup phase in the future. This is because, when machine learning algorithms determine the optimal parameters and operating conditions, they can be integrated into the control mechanisms of the systems, eliminating the initial installation and operating costs of components such as flow meters in experimental setups. In this study, which is the first in the literature in terms of the application of artificial intelligence in a three-stage cascade refrigeration system, the evaporator temperature, the condenser temperature of the low-temperature cycle, the condenser temperature of the medium-temperature cycle, the condenser temperature of the high-temperature cycle and the cascade heat exchanger (CHX) temperature difference were used as input parameters, while COP, exergy

efficiency, total compressor power consumption and total exergy destruction were used as outputs. Multilayer Perceptron methodology and the outcomes obtained in this study will contribute significantly to the optimal design and performance forecasting of the three-stage cascade refrigeration system, as well as to the ensuing experimental trials. This study addresses a critical aspect of refrigeration technology, focusing on the enhancement of three-stage cascade refrigeration systems from both thermodynamic and machine learning perspectives—a topic that has received limited attention in the existing literature. This study serves as a foundational work for future research in ultra-low temperature refrigeration area, presenting a structured methodology for system analysis and incorporating machine learning models for optimization purposes.

1.1. Utilized refrigerants

As awareness of global warming and ozone depletion issues increases as well as the regulations about limitations of old generation refrigerants, research on alternative refrigerants has gained significant attention in recent years. The discovery of ozone depletion in the atmospheric stratosphere, caused by synthetic chlorofluorocarbon (CFC) and hydrochlorofluorocarbon (HCFC) type refrigerants, led to the establishment of the Montreal Protocol and its subsequent amendments, ultimately resulting in the permanent ban of these substances (Roy and Mandal 2019). CFCs were banned under the Montreal Protocol in 1987. Additionally, Kyoto Protocol signed in 1997 scheduled HCFCs phase-out between 2020 and 2030, and hydrofluorocarbons (HFCs) phased out between 2025 and 2040 (Das, Pektezel, and Alic 2022). The Paris Agreement of 2015 and the Kigali Amendment to the Montreal Protocol in 2016 emphasized the need for substantial reductions in the use of HFCs (Das and Pektezel 2022). Although ultra-low temperature refrigeration is not specifically regulated by emissions reduction protocols, there is an immediate need to identify low-GWP alternative refrigerants to mitigate its environmental impact (Liu, Bacellar, and Aute 2023).

One of the most important factors affecting the operating performance of refrigeration systems is the selection of the refrigerant to be used. Selecting the appropriate refrigerant for CRS can improve the cooling capacity and COP of the system. Thus, the operating life of the system can be extended, and the environmental impact can be minimized. Numerous research institutions have made substantial progress in identifying refrigerant replacements, particularly for low-temperature circuits (LTC), focusing on options with zero ozone depletion potential (ODP) and low global warming potential (GWP) (Sun et al. 2016). In the fields of refrigeration and chemical engineering, researchers have identified two primary approaches for mitigation and alternative solutions (Sun et al. 2019b). The first approach involves the continued development of synthetic refrigerants with low GWP (Mota-Babiloni, Makhnatch, and Khodabandeh 2017). The second approach focuses on the utilization of natural refrigerants, including R744, R717, R600a, and R290 (Harby 2017).

The high-temperature cycle (HTC) of a CRS is typically charged with intermediate-temperature refrigerants, which generally have a normal boiling point (NBP) ranging from 0 °C to −60 °C such as R404A, R1270, R290, and R717 (Sun et al. 2019a). For LTC, refrigerants with NBP lower than −60 °C are preferred.

R1150 has the chemical formula of C_2H_4, and it is known as ethylene. It is suitable for very low temperature industrial refrigeration applications since it has a low boiling point. Its application area includes natural gas liquefaction, low temperature storage and freeze drying. R170 is known as ethane and has the chemical formula of C_2H_6. R-170 exhibits advantageous thermodynamic and transport properties, making it an effective cryogenic refrigerant (Zhang et al. 2023). It has also been noted that R170 exhibits an optimal lower pressure ratio along with superior isentropic and volumetric efficiency compared to other working fluids (Mota-Babiloni et al. 2020). R170 can be utilized in industrial and commercial refrigeration systems where low temperatures are required. R744 refrigerant, also known as carbon dioxide, has the chemical formula of CO_2. R744, a natural refrigerant with excellent thermo-physical properties, offers a cost-effective, nontoxic, and non-flammable alternative that effectively mitigates issues related to direct emissions, while its superior performance in cold climates enables it to surpass high-GWP refrigerants and substantially reduce greenhouse gas emissions (Gullo, Elmegaard, and Cortella 2016). R-744 has low liquid density, which contributes to a reduced system size and lower refrigerant charge requirements. R-744 provides a high refrigeration capacity of 22,600 kJ/kg at 0 °C, which is 5 to 22 times greater than that of other synthetic and natural refrigerants (Abas et al. 2018). The primary obstacle to the widespread adoption of R744 as a refrigerant is its need for extremely high condensation pressure, approximately 200 atmospheres, which increases the costs associated with designing systems capable of withstanding such pressures (Alsouda et al. 2023). R744 has been used in different kind of vapor compression applications for about 130 years (Uddin and Saha 2022). R1270 refrigerant has the chemical formula of C_3H_6, and it is also named as propylene. R1270 refrigerant's application area include commercial refrigeration systems, industrial refrigeration, small and large air conditioning systems for commercial and industry purposes. The thermodynamic properties of R-1270 enable efficient energy utilization, while its compatibility with air conditioning system components, low operational cost, excellent thermal conductivity, and requirement for smaller pipe dimensions make it a highly practical refrigerant (Sumardi, Nahadi, and Mutaufiq 2020). The major drawback of R1270 is its flammability. However, the allowable greatest amount of charge for flammable refrigerants to be used in commercial refrigeration systems has been remarkably risen with respect to International Electrotechnical Commission 60335–2 89:2019 standard (Zhang et al. 2024). R717 with the chemical formula of NH_3 is known as ammonia. R717 is a natural refrigerant. It has

Table 1. Properties of the refrigerants used in analyses (Mota-Babiloni et al. 2020).

Cycle	Refrigerant	ODP	$GWP_{100\text{-}yr}$ (CO_2-eq)	ASHRAE safety group	NBP (°C)	Molecular weight (kg mol^{-1})	Critical temperature (°C)	Critical pressure (MPa)
LTC	R1150	0	4	A3	−103.77	28.05	9.2	5.04
MTC	R170	0	5.5	A3	−88.58	30.07	32.17	4.87
MTC	R744	0	1	A1	−78.46	44.01	30.98	7.38
HTC	R1270	0	<1	A3	−47.62	42.08	91.06	4.55
HTC	R717	0	0	B2L	−33.33	17.03	132.25	11.33
HTC	R1234yf	0	<1	A2L	−29.45	114.04	94.7	3.38

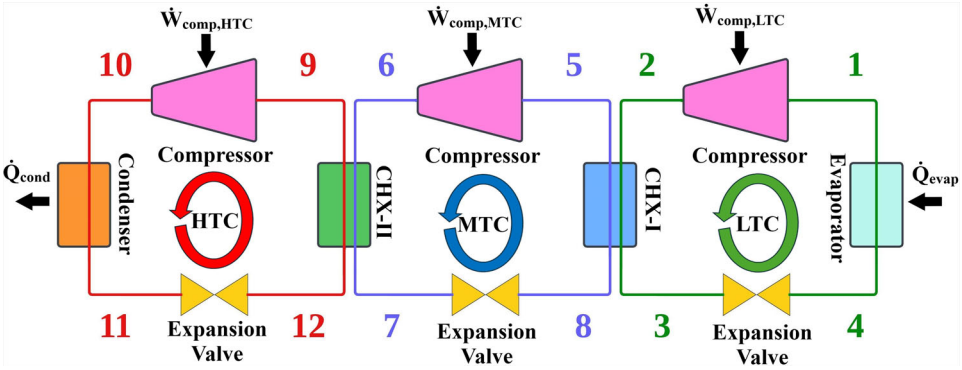

Fig. 1. Schematic diagram of three-stage cascade refrigeration system.

been used as an accepted refrigerant in the world for over a century. R717 has gained widespread recognition for its favorable thermodynamic properties, such as high efficiency, affordability, availability, and minimal environmental impact, while its high latent heat of vaporization and low flow rate requirements make it a preferred choice for large-scale refrigeration applications (Alsouda et al. 2023). R717 has toxicity property which makes its application limited in domestic applications and automobile sector usage (Uddin and Saha 2022). Although R717 is toxic, its strong odor serves as a natural warning sign for potential leaks. R1234yf has the chemical formula of 2,3,3,3-tetrafluoroprop-1-ene. R-1234yf has been uniquely developed as a replacement for R-134a due to their comparable thermophysical properties, while also offering advantages such as nontoxicity, non-mutagenicity, and a significantly higher minimum ignition energy compared to alternatives like R-32 (Vuppaladadiyam et al. 2022). R1234yf refrigerant is especially an alternative for R134a in automobile air conditioning applications. But, its application area also include cold storage, commercial ice machines, food retail like supermarket systems, and industrial process refrigeration. Table 1 shows properties of the refrigerant used in the study.

2. Three-stage cascade refrigeration system

Three-stage cascade refrigeration systems are widely employed in industrial refrigeration and can effectively meet the cooling requirements for temperatures below −80 °C. In addition, refrigeration applications below −80 °C evaporation temperature have been also gradually becoming important in the fields such as high purity oxygen and nitrogen production with cryogeny, precipitation hardening of particular alloy steel, petroleum steam liquefaction, biomedicine, and cryotherapy where patients are subjected to very cold conditions (Hamzaoui, Tiachacht, and Hadiouche 2024b; Sun et al. 2019a; Sun and Wang 2022).

The schematic diagram of the three-stage cascade refrigeration system is presented in Figure 1. The system primarily consists of an evaporator, three compressors, three expansion valves, two cascade heat exchangers, and a condenser. The necessary ultra-low room temperature is achieved through the low-temperature refrigerant gas flowing through the evaporator in the low-temperature cycle. The compressor in the LTC increases the temperature and pressure of the refrigerant fluid, sending it to the CHX-I. This cascade heat exchanger serves as the condenser for the LTC cycle, while it acts as the evaporator for the medium-temperature cycle (MTC). Subsequently, the refrigerant gas passes through the expansion valve, reducing its pressure and temperature. In the MTC cycle, heat is extracted from the condenser of the LTC cycle via the CHX-I. Then, compression occurs in the compressor located between points 5 and 6. The CHX-II serves as the condenser for the MTC cycle and as the evaporator for the HTC. The fluid passes through the expansion valve located between points 7 and 8, reducing its temperature and pressure. In the evaporator of the HTC cycle, heat is absorbed from the condenser of the MTC cycle, meaning that the heat rejected and absorbed are equal. Afterward, the compressor between points 9 and 10

increases the temperature and pressure of the fluid. Finally, heat is rejected to the environment through the condenser between points 10 and 11. The refrigerant then passes through the expansion valve, reducing its temperature and pressure, thereby completing the cycle.

2.1. Thermodynamic modelling of the system

Thermodynamic modeling of the system was carried out using EES (Klein 2013). The following assumptions have been utilized in the design of the system.

1. The components of the system are assumed to operate under steady state conditions.
2. Pressure drops as well as heat losses and gains are neglected for the entire piping.
3. Kinetic and potential energy changes in system components are ignored.
4. Power consumptions of the condenser and the evaporator fans are neglected.
5. Adiabatic compression and expansion are assumed for compressors and expansion valves.
6. There is no subcooling at the exit of the condensers, namely the quality of the points 3, 7, and 11 are zero.
7. There is no superheating at the exit of the evaporators, namely the quality of the points 1, 5, and 9 are equal to one.
8. 5 °C of temperature difference was assumed between the evaporator temperature and the refrigerated space temperature.
9. Heat sink temperature of the condenser is assumed to be equal to the ambient temperature. In addition, ambient temperature and pressure are considered as 25 °C and 101.325 kPa, respectively.
10. Air is assumed as the heat exchanging fluid with the refrigerant in both the condenser and the evaporator.

COP of the three-stage cascade refrigeration system is calculated using Equation 1.

$$\mathrm{COP} = \frac{\dot{Q}_{evap}}{\dot{W}_{comp,total}} \tag{1}$$

where total compressor power consumption is defined with Equation 2.

$$\dot{W}_{comp,total} = \dot{W}_{comp,LTC} + \dot{W}_{comp,MTC} + \dot{W}_{comp,HTC} \tag{2}$$

Exergy of each system point can be defined with the Equation 3.

$$e_i = (h_i - h_0) - T_0(s_i - s_0) \tag{3}$$

Flow exergy of system points can be calculated by multiplying exergy with mass flow rate.

$$\dot{E}_i = \dot{m}_i e_i \tag{4}$$

Total exergy destruction is given with Equation 5.

$$\dot{E}_{dest,\,total} = \dot{E}_{dest,\,evap} + \dot{E}_{dest,\,comp,\,LTC} + \dot{E}_{dest,\,CHX,\,I} + \dot{E}_{dest,\,valve,\,LTC} + \dot{E}_{dest,\,comp,\,MTC} + \dot{E}_{dest,CHX,II} + \dot{E}_{dest,valve,MTC} + \dot{E}_{dest,comp,HTC} + \dot{E}_{dest,cond} + \dot{E}_{dest,valve,HTC} \tag{5}$$

Exergy efficiency of the system is demonstrated with Equation 6.

$$\eta_{ex} = 1 - \left(\frac{\dot{E}_{dest,total}}{\dot{W}_{comp,total}}\right) \tag{6}$$

Energy and exergy equations of all system components are given in Table 2. The isentropic efficiency formula used for the compressors in this study has been applied in many studies in the literature to be valid for various gases and different stages of cascade refrigeration systems (Chen et al. 2023; Hamzaoui, Tiachacht, and Hadiouche 2024b; Singha et al. 2024; Sun et al. 2019a, 2019b; Ye et al. 2024a; 2024b).

Some input parameters are necessary to solve the mathematical model of the system. Design parameters of the system are presented in Table 3. Mechanical and electrical efficiency values for the compressors were selected to be consistent with the previous studies (Faruque, Uddin, et al. 2022; Ji et al. 2024; Nabil et al. 2023). The input values required for economic analysis were taken from similar studies in literature (Kayes et al. 2024; Nabil et al. 2023).

2.2. Validation of the generated model

In thermodynamic analysis, it is essential to validate the accuracy of the created model by testing it against well-established models in literature. In this context, the input parameters of the three-stage cascade refrigeration system given in Table 4 and designed by Sun et al. (2019a) have been tested in the EES model developed in this study. The results are presented in Figure 2. Upon examining Figure 2, it can be seen that the model developed in this study shows high agreement with the reference model, thereby confirming the accuracy of the model.

3. Multilayer perceptron machine learning approach

Artificial Neural Networks (ANNs) have attracted considerable attention due to their ability to emulate the functioning of the human brain and their efficiency in addressing complex problems (Afzal et al. 2023). Multilayer Perceptron (MLP) is an enhanced version of ANN designed for engineering applications and energy systems; it is regarded as a feed-forward neural network that employs a supervised learning approach with backpropagation for training (Mosavi et al. 2019). MLP is a robust type of nonlinear statistical model made up of three different types of layers: input, hidden, and output where each layer is entirely connected to the following one (Orrù et al. 2020). MLP is an artificial neural network architecture aimed at estimating a numerical target value by processing inputs through multiple layers of nonlinear transformations (Tatar 2025). The input layer is the initial layer, containing the input variables for processing, while the final or output layer computes the value of the output or desired parameter based on the data obtained from the hidden layers; to complete the MLP structure, the hidden layers should be positioned between the input and output layers (Jin et al. 2022).

Table 2. Thermodynamic equations of system components.

Component	*Energy and exergy formulations*
Evaporator	$\dot{Q}_{evap} = \dot{m}_{LTC}(h_1 - h_4)$
	$\dot{E}_{dest,evap} = \dot{E}_4 - \dot{E}_4 - \dot{E}_{Q,evap}$
	$\dot{E}_{Q,evap} = \left(\frac{T_0}{T_L} - 1\right)\dot{Q}_{evap}$
LTC Compressor	$\dot{W}_{comp,LTC} = \frac{\dot{m}_{LTC}(h_2 - h_1)}{\eta_m \eta_e}$
	$\eta_{comp,LTC} = 0.874 - 0.0135\left(\frac{P_2}{P_1}\right) = \frac{h_{2s} - h_1}{h_2 - h_1}$
	$\dot{E}_{dest,comp,LTC} = \dot{E}_1 - \dot{E}_2 + \dot{W}_{comp,LTC}$
Cascade Heat Exchanger I	$\dot{m}_{LTC}(h_2 - h_3) = \dot{m}_{MTC}(h_5 - h_8)$
	$\dot{E}_{dest,CHX,I} = \dot{E}_2 + \dot{E}_8 - \dot{E}_3 - \dot{E}_5$
LTC Expansion Valve	$h_3 = h_4$
	$\dot{E}_{dest,valve,LTC} = \dot{E}_3 - \dot{E}_4$
MTC Compressor	$\dot{W}_{comp,MTC} = \frac{\dot{m}_{MTC}(h_6 - h_5)}{\eta_m \eta_e}$
	$\eta_{comp,MTC} = 0.874 - 0.0135\left(\frac{P_6}{P_5}\right) = \frac{h_{6s} - h_5}{h_6 - h_5}$
	$\dot{E}_{dest,comp,MTC} = \dot{E}_5 - \dot{E}_6 + \dot{W}_{comp,MTC}$
Cascade Heat Exchanger II	$\dot{m}_{MTC}(h_6 - h_7) = \dot{m}_{HTC}(h_9 - h_{12})$
	$\dot{E}_{dest,CHX,II} = \dot{E}_6 + \dot{E}_{12} - \dot{E}_7 - \dot{E}_9$
MTC Expansion Valve	$h_7 = h_8$
	$\dot{E}_{dest,valve,MTC} = \dot{E}_7 - \dot{E}_8$
HTC Compressor	$\dot{W}_{comp,HTC} = \frac{\dot{m}_{HTC}(h_{10} - h_9)}{\eta_m \eta_e}$
	$\eta_{comp,HTC} = 0.874 - 0.0135\left(\frac{P_{10}}{P_9}\right) = \frac{h_{10s} - h_9}{h_{10} - h_9}$
	$\dot{E}_{dest,comp,HTC} = \dot{E}_9 - \dot{E}_{10} + \dot{W}_{comp,HTC}$
Condenser	$\dot{Q}_{cond} = \dot{m}_{HTC}(h_{10} - h_{11})$
	$\dot{E}_{dest,cond} = \dot{E}_{10} - \dot{E}_{11} - \dot{E}_{Q,cond}$
	$\dot{E}_{Q,cond} = \left(1 - \frac{T_0}{T_H}\right)\dot{Q}_{cond}$
HTC Expansion Valve	$h_{11} = h_{12}$
	$\dot{E}_{dest,valve,HTC} = \dot{E}_{11} - \dot{E}_{12}$

Table 3. Design parameters of the model.

Parameter	Input value	Range
$\dot{Q}_{evap}$	10 kW	–
$\Delta T_{CHX,I}$	5 °C	3 °C to 7 °C
$\Delta T_{CHX,II}$	5 °C	–
T_{evap}	−100 °C	−115 °C to −85 °C
$T_{cond,LTC}$	−60 °C	−75 °C to −45 °C
$T_{cond,MTC}$	−10 °C	−20 °C to 5 °C
$T_{cond,HTC}$	40 °C	30 °C to 50 °C
η_m	0.9	–
η_e	0.95	–
Plant lifetime, n	15 years	–
Maintenance factor, φ	1.06	–
Interest rate, i	%14	–
Annual operation hour, N	4266 h	–
Emission factor, μ_{CO_2}	0.968 kg/kWh	–
Cost related with avoiding CO_2, C_{CO_2}	0.09 $/kg release of CO_2	–
Electricity cost, $\propto_{electricity}$	0.09 $/kWh	–
Overall heat transfer coefficient, U	30 $Wm^{-2}K^{-1}$ for evaporator	–
	40 $Wm^{-2}K^{-1}$ for HTC condenser	–
	1000 $Wm^{-2}K^{-1}$ for cascade heat exchangers	–

Table 4. Utilized parameters for the validation of the model (Sun et al. 2019a).

Parameter	Value
Cooling Capacity, $\dot{Q}_{evap}$	10 kW
Evaporator Temperature, T_{evap}	−100 °C
LTC Condensation Temperature, $T_{cond,LTC}$	−85 °C, −80 °C, −75 °C, −70 °C, −65 °C, −60 °C, −55 °C, −50 °C, −45 °C
MTC Condensation Temperature, $T_{cond,MTC}$	−28.4 °C, −25.6 °C, −23 °C, −20.6 °C, −18.4 °C, −16.2 °C, −14 °C, −12 °C, −10.2 °C
HTC Condensation Temperature, $T_{cond,HTC}$	40 °C
Cascade Temperature Difference, $\Delta T_{CHX,I}$ and $\Delta T_{CHX,II}$	5 °C
Isentropic Efficiency of the Compressors	0.874–0.0135·Pressure Ratio
Superheating Degree of LTC, MTC and HTC	12 °C, 12 °C, 5 °C
Refrigerant	R1150/R170/R161

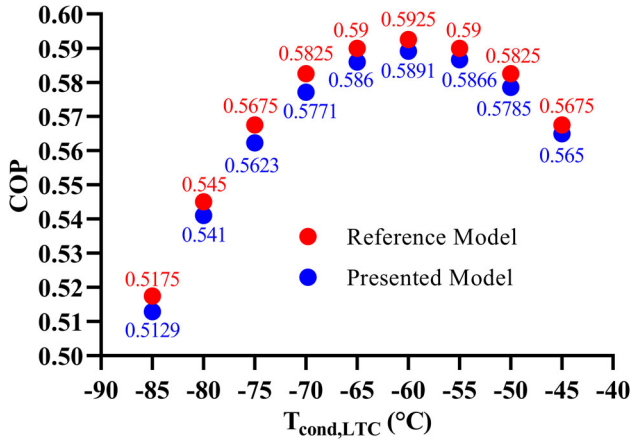

Fig. 2. Validation of the model.

Table 5 presents the models created for COP estimation. A total of 18 different network structures were used in COP optimization. The models were generated by altering the number of neurons in the hidden layer and the number of hidden layers. Upon analyzing the results, it can be concluded that the model with the least error in both the training and test sets is model number 16, and therefore, this model can be considered the optimal one for COP prediction.

Upon reviewing the results obtained from different network structures for compressor power consumption estimation, as shown in Table 6, it can be concluded that the 5-7-1-1 network structure resulted in the lowest error and is therefore considered the optimal model.

Table 7 presents the MLP models created for exergy efficiency estimation. Upon examining the models created with different numbers of neurons in the hidden layer and varying numbers of hidden layers, it can be concluded that model number 16 exhibited the best prediction performance. Therefore, the network structure represented by model 16 was utilized in the analysis.

The error values for 18 different models created to optimize the total exergy destruction prediction performance using MLP are presented in Table 8. The results reveal that the 5-7-1-1 configuration is the most successful network structure.

The relatively higher prediction errors in individual test set data points may be attributed to a few factors. First, the inherent complexity of the three-stage cascade refrigeration system, especially at ultra-low temperatures, introduces nonlinear behaviors that may not be fully captured by the current MLP model configuration. Additionally, the variability in input parameters obtained from EES analyses, such as fluctuating LTC, MTC and HTC condenser temperatures, changing evaporator temperatures, and varying temperature difference values of cascade heat exchanger, could contribute to the observed discrepancies.

Figure 3 shows the MLP network structure used for all predicted parameters, including total exergy destruction, COP, exergy efficiency, and total compressor power consumption. Since the 5-7-1-1 configuration resulted in the least error across all prediction parameters, this sequence was used in the predictions.

4. Results and discussion

The findings obtained in the study are discussed under three main subheadings: parametric analysis results, which present the thermodynamic analysis outcomes, machine learning results, which include the MLP prediction performance, and economic analysis results, which present total cost of the system.

4.1. Parametric analysis results

Figure 4a,b show the effect of evaporator temperature on COP for all refrigerant groups used. It can be seen from the figure that increasing the evaporator temperature leads to an increase in COP. For example, for the R1150/R744/R717 group, increasing the evaporator temperature from −115 °C to −85 °C resulted in an increase in COP from 0.35 to 0.63. When comparing the used refrigerants, it can be stated that the R1150/R170/R717 group provides the highest COP. With this group, the highest COP value obtained in the parametric analysis at an evaporator temperature of −85 °C was 0.65. In addition, the lowest COP value in the system was

Table 5. MLP models for COP.

Model No	Network structure	Training MAE & RMSE for COP	Test MAE & RMSE for COP
1	5-2-1-1	0.0044 & 0.0052	0.0046 & 0.0055
2	5-2-2-1-1	0.0046 & 0.0054	0.0050 & 0.0057
3	5-2-2-2-1-1	0.0048 & 0.0060	0.0059 & 0.0074
4	5-3-1-1	0.0038 & 0.0045	0.0041 & 0.0050
5	5-3-3-1-1	0.0038 & 0.0048	0.0043 & 0.0052
6	5-3-3-3-1-1	0.0042 & 0.0052	0.0044 & 0.0056
7	5-4-1-1	0.0034 & 0.0043	0.0035 & 0.0042
8	5-4-4-1-1	0.0040 & 0.0048	0.0042 & 0.0052
9	5-4-4-4-1-1	0.0042 & 0.0051	0.0045 & 0.0054
10	5-5-1-1	0.0031 & 0.0040	0.0032 & 0.0040
11	5-5-5-1-1	0.0041 & 0.0051	0.0042 & 0.0053
12	5-5-5-5-1-1	0.0015 & 0.0020	0.0021 & 0.0023
13	5-6-1-1	0.0010 & 0.0011	0.0011 & 0.0012
14	5-6-6-1-1	0.0042 & 0.0051	0.0045 & 0.0055
15	5-6-6-6-1-1	0.0041 & 0.0050	0.0046 & 0.0054
16	5-7-1-1	0.0004 & 0.0006	0.0006 & 0.0007
17	5-7-7-1-1	0.0040 & 0.0046	0.0042 & 0.0051
18	5-7-7-7-1-1	0.0013 & 0.0018	0.0017 & 0.0020

Table 6. MLP models for $\dot{W}_{comp,total}$.

Model No	Network structure	Training MAE & RMSE for Ẇcomp,total	Test MAE & RMSE for Ẇcomp,total
1	5-2-1-1	0.0824 & 0.0972	0.0890 & 0.1070
2	5-2-2-1-1	0.0883 & 0.1168	0.1172 & 0.1471
3	5-2-2-2-1-1	0.0886 & 0.1135	0.1106 & 0.1390
4	5-3-1-1	0.0635 & 0.0827	0.0640 & 0.0846
5	5-3-3-1-1	0.0647 & 0.0756	0.0655 & 0.0789
6	5-3-3-3-1-1	0.0988 & 0.1151	0.0905 & 0.1114
7	5-4-1-1	0.0924 & 0.1042	0.0944 & 0.1099
8	5-4-4-1-1	0.0296 & 0.0371	0.0354 & 0.0475
9	5-4-4-4-1-1	0.0609 & 0.0793	0.0782 & 0.1051
10	5-5-1-1	0.0257 & 0.0296	0.0269 & 0.0326
11	5-5-5-1-1	0.0261 & 0.0336	0.0293 & 0.0398
12	5-5-5-5-1-1	0.0244 & 0.0309	0.0285 & 0.0383
13	5-6-1-1	0.0238 & 0.0284	0.0265 & 0.0321
14	5-6-6-1-1	0.0475 & 0.0541	0.0476 & 0.0555
15	5-6-6-6-1-1	0.0291 & 0.0369	0.0347 & 0.0457
16	5-7-1-1	0.0147 & 0.0188	0.0193 & 0.0268
17	5-7-7-1-1	0.0369 & 0.0434	0.0390 & 0.0482
18	5-7-7-7-1-1	0.0415 & 0.0491	0.0426 & 0.0520

found to be 0.34 when using R1150/R744/R1234yf at an evaporator temperature of −115 °C. In the experimental study on the cascade refrigeration system conducted by Bingming et al. (2009), it was found that the COP increases with the rise in evaporator temperature. Furthermore, it was stated that there is an almost linear relationship between the evaporator temperature and COP, as observed in this study.

Figure 4c,d show the effect of evaporator temperature on total compressor power consumption. Upon examining the figures, it is clear that increasing the evaporator temperature results in a decrease in compressor consumption. Similar findings were reported by Hamzaoui, Tiachacht, and Hadiouche (2024b). For example, for the R1150/R170/R1270 group, increasing the evaporator temperature from −115 °C to −85 °C reduced the compressor consumption by 44%. Among the refrigerant groups used, the highest consumption occurred for R1150/R744/R1234yf at −115 °C with 29.64 kW, while the lowest consumption occurred for R1150/R170/R717 at −85 °C with 15.45 kW. In the experimental study on the cascade refrigeration system, Jeon

Table 7. MLP models for η_{ex}.

Model No	Network structure	Training MAE & RMSE for ηex	Test MAE & RMSE for ηex
1	5-2-1-1	0.0025 & 0.0034	0.0028 & 0.0035
2	5-2-2-1-1	0.0024 & 0.0033	0.0030 & 0.0038
3	5-2-2-2-1-1	0.0025 & 0.0031	0.0028 & 0.0035
4	5-3-1-1	0.0021 & 0.0028	0.0025 & 0.0034
5	5-3-3-1-1	0.0022 & 0.0027	0.0027 & 0.0032
6	5-3-3-3-1-1	0.0021 & 0.0029	0.0026 & 0.0033
7	5-4-1-1	0.0015 & 0.0021	0.0015 & 0.0021
8	5-4-4-1-1	0.0005 & 0.0006	0.0006 & 0.0007
9	5-4-4-4-1-1	0.0020 & 0.0026	0.0021 & 0.0027
10	5-5-1-1	0.0006 & 0.0007	0.0006 & 0.0007
11	5-5-5-1-1	0.0020 & 0.0026	0.0028 & 0.0035
12	5-5-5-5-1-1	0.0010 & 0.0011	0.0009 & 0.0011
13	5-6-1-1	0.0005 & 0.0007	0.0006 & 0.0008
14	5-6-6-1-1	0.0003 & 0.0004	0.0004 & 0.0005
15	5-6-6-6-1-1	0.0004 & 0.0006	0.0006 & 0.0007
16	5-7-1-1	0.0002 & 0.0003	0.0003 & 0.0003
17	5-7-7-1-1	0.0015 & 0.0021	0.0015 & 0.0022
18	5-7-7-7-1-1	0.0003 & 0.0005	0.0004 & 0.0005

Table 8. MLP models for $\dot{E}_{dest,total}$.

Model No	Network structure	Training MAE & RMSE for Ėdest,total	Test MAE & RMSE for Ėdest,total
1	5-2-1-1	0.0795 & 0.1061	0.0969 & 0.1299
2	5-2-2-1-1	0.0860 & 0.1134	0.1121 & 0.1410
3	5-2-2-2-1-1	0.0888 & 0.1112	0.0987 & 0.1262
4	5-3-1-1	0.0604 & 0.0834	0.0799 & 0.1049
5	5-3-3-1-1	0.0621 & 0.0716	0.0623 & 0.0712
6	5-3-3-3-1-1	0.1070 & 0.1195	0.1018 & 0.1165
7	5-4-1-1	0.0699 & 0.0820	0.0722 & 0.0859
8	5-4-4-1-1	0.0251 & 0.0308	0.0306 & 0.0396
9	5-4-4-4-1-1	0.0670 & 0.0852	0.0862 & 0.1087
10	5-5-1-1	0.0398 & 0.0435	0.0405 & 0.0451
11	5-5-5-1-1	0.0243 & 0.0297	0.0269 & 0.0348
12	5-5-5-5-1-1	0.0255 & 0.0306	0.0288 & 0.0366
13	5-6-1-1	0.0234 & 0.0272	0.0257 & 0.0293
14	5-6-6-1-1	0.0376 & 0.0425	0.0389 & 0.0446
15	5-6-6-6-1-1	0.0355 & 0.0427	0.0402 & 0.0491
16	5-7-1-1	0.0178 & 0.0214	0.0194 & 0.0241
17	5-7-7-1-1	0.0326 & 0.0378	0.0345& 0.0427
18	5-7-7-7-1-1	0.0279 & 0.0336	0.0310 & 0.0385

(2021) found that as the evaporator temperature increases, the total compressor power consumption decreases. This observation shows that the results obtained in this study are consistent with the experimental studies in the literature.

Figure 5a,b show the effect of evaporator temperature on the exergy efficiency of the system. Upon examining the results, it is understood that increasing the evaporator temperature leads to an increase in exergy efficiency. Similar results were reached by Sun et al. (2019a). This increase starts more sharply from −115 °C and begins to level off starting from −90 °C. For example, for the R1150/R744/R1270 group, increasing the evaporator temperature from −115 °C to −85 °C resulted in an increase in exergy efficiency from 0.29 to 0.33, causing a 13.8% increase. Among all refrigerant groups, the group with the highest exergy efficiency was R1150/R170/R717. Using this group, the highest exergy efficiency of 0.35 was achieved at −85 °C. The lowest exergy efficiency, however, was observed with R1150/R744/R1234yf at −115 °C, with a value of 0.28.

Figure 5c,d show the effect of evaporator temperature on total exergy destruction. The results indicate that as the evaporator temperature increases, total exergy destruction

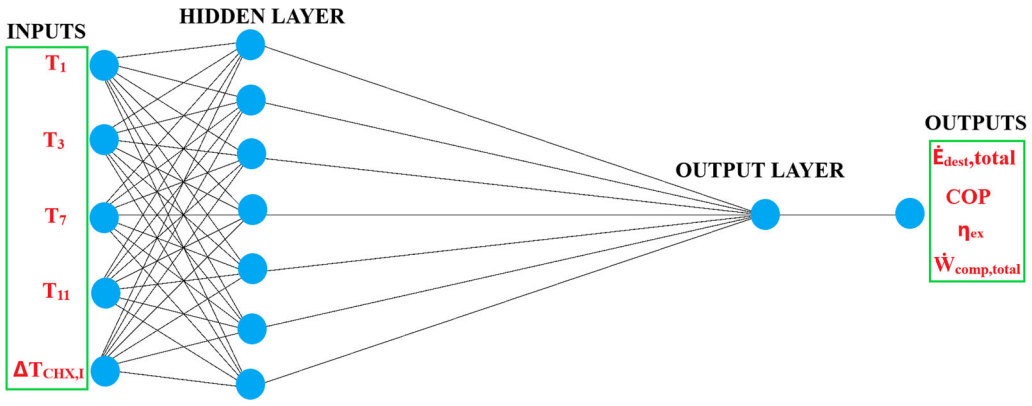

Fig. 3. MLP network structure for all predicted parameters.

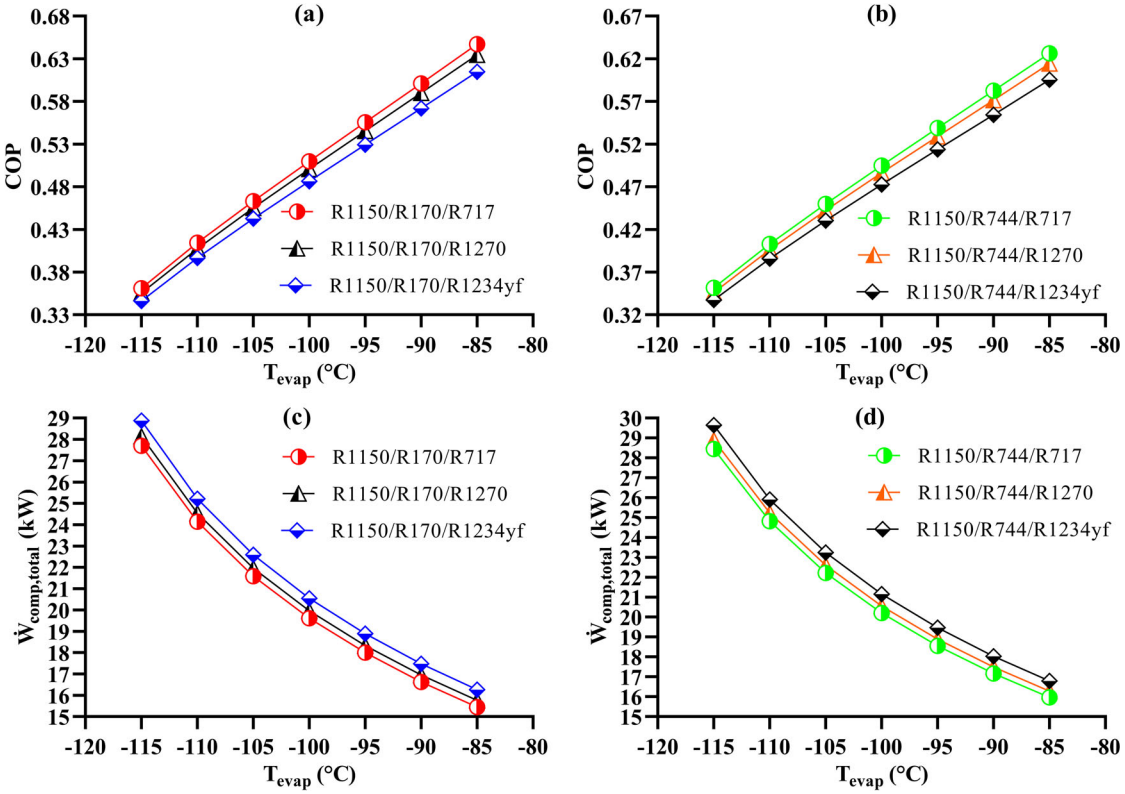

Fig. 4. Effect of T_{evap} on COP and $\dot{W}_{comp,total}$.

decreases. This makes sense because, in the temperature ranges where exergy efficiency increases, it is thermodynamically expected for exergy destruction to decrease as well. As an example, when using R1150/R170/R1234yf, increasing the evaporator temperature from −115 °C to −85 °C results in a reduction of total exergy destruction from 20.6 kW to 10.8 kW. The analysis results pointed to the R1150/R744/R1234yf group as the refrigerant responsible for the highest exergy destruction in the system, with a maximum exergy destruction of 21.4 kW at −115 °C. For minimum exergy destruction, the R1150/R170/R717 group stood out with a destruction of 10 kW at −85 °C.

Figure 6a,b illustrate the effect of LTC cycle condenser temperature on the COP. The figure shows that as $T_{cond,TLC}$ increases, the COP rises to a peak value at −55 °C and then begins to decrease. Similar tendency was determined by Walid Faruque, Uddin, et al. (2022). For example, for the R1150/R744/R1234yf group, the COP reaches a minimum value of 0.4 at −75 °C and a maximum value of 0.48 at −55 °C, after which it starts to decrease, reaching 0.46 at −45 °C. When comparing fluid groups, it can be stated that the R1150/R170/R717 group provides the highest COP across all $T_{cond,TLC}$ temperatures. In their experimental study on the cascade refrigeration system, Sanz-Kock et al. (2014) observed that as the condenser temperature of the low-temperature cycle increases, the COP also increases and then reaches a peak point, similar to what was identified in this study. In their experimental study, Dopazo and Fernández-

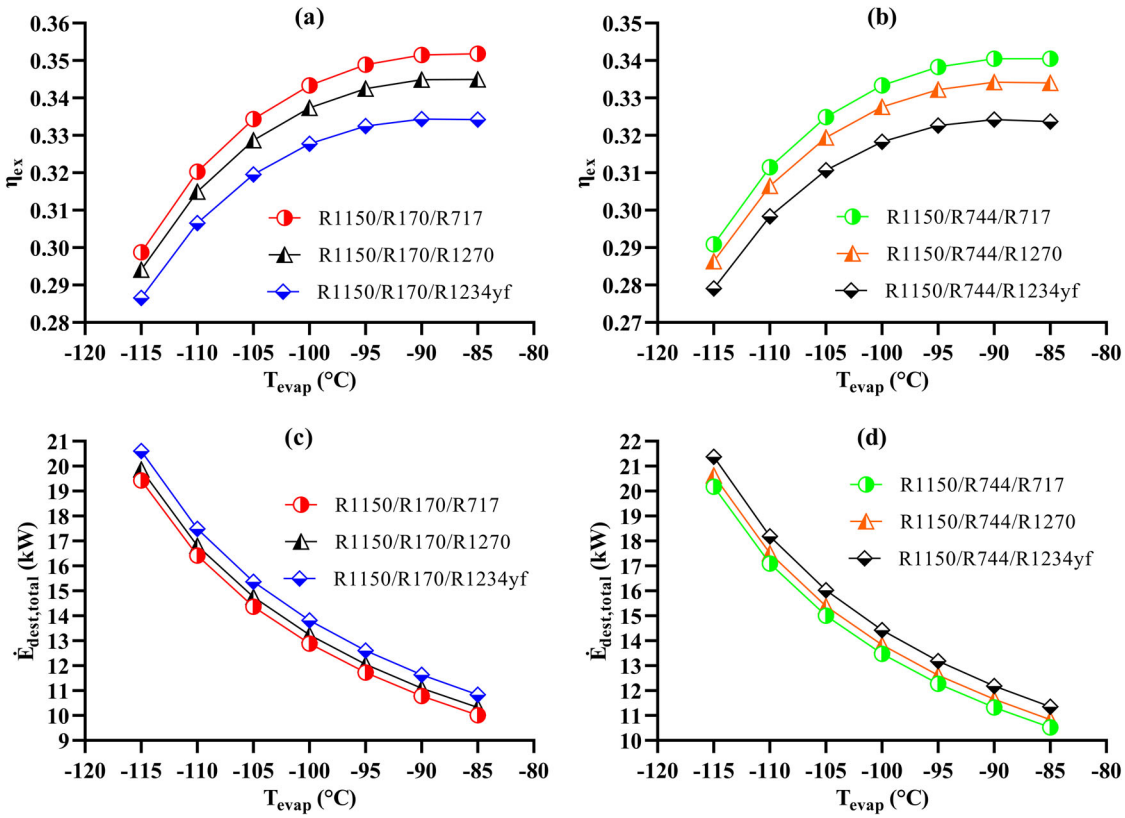

Fig. 5. Effect of T_{evap} on η_{ex} and $\dot{E}_{dest,total}$.

Seara (2011) found that as the condenser temperature of the low-temperature cycle in the cascade refrigeration system increases, the COP initially rises, then reaches a peak point, and subsequently starts to decline. This observation indicates that the results obtained in this study are consistent with the experimental studies in the literature.

Figure 6c,d present the effect of the LTC condenser temperature variation on the total compressor consumption. As the $T_{cond,TLC}$ temperature increases, the compressor consumption decreases up to a certain point, after which it begins to rise, as shown in the figure. For instance, for the R1150/R744/R717 group, the compressor consumption at −75 °C is 23.64 kW, which decreases to 20 kW at −55 °C, showing a reduction of 15.4%, and then increases to 20.48 kW at −45 °C. When comparing refrigerants, the R1150/R744/R1234yf group is found to cause the highest consumption at all $T_{cond,TLC}$ temperatures.

Figure 7a,b demonstrate the impact of the LTC cycle condenser temperature on exergy efficiency. The data reveals that as $T_{cond,TLC}$ increases, exergy efficiency initially rises, peaking at −55 °C, before subsequently declining. For instance, in the case of the R1150/R170/R1270 group, the exergy efficiency reaches its minimum value of 0.31 at −75 °C and its maximum value of 0.34 at −55 °C, after which it decreases to 0.32 at −45 °C. A comparison of fluid groups indicates that the R1150/R170/R717 group consistently delivers the highest exergy efficiency across the full range of $T_{cond,TLC}$ temperatures.

Figure 7c,d illustrate the effect of the LTC condenser temperature change on total exergy destruction. As the $T_{cond,TLC}$ temperature increases, exergy destruction decreases up to a certain point, after which it starts to increase, as depicted in the figure. For example, for the R1150/R744/R1270 group, the exergy destruction at −75 °C is 17.3 kW, which decreases to 13.62 kW at −55 °C, representing a reduction of 21.3%, and then rises to 14.1 kW at −45 °C. When comparing refrigerants, the R1150/R744/R1234yf group is found to result in the highest exergy destruction across all $T_{cond,TLC}$ temperatures.

Figure 8a,b show the variation in COP resulting from changes in the MTC condenser temperature between −20 °C and 5 °C. The obtained results indicate that as $T_{cond,MTC}$ increases, COP initially exhibits a slight increase, after which it begins to decrease. For example, for the R1150/R170/R717 group, the COP is 0.5 at −20 °C and rises to 0.51 at −15 °C, but then starts to decrease, reaching 0.46 at 5 °C.

Figure 8c,d illustrate the effect of the increase in MTC condenser temperature from −20 °C to 5 °C on total compressor power consumption. As $T_{cond,MTC}$ increases, it can be observed that compressor consumption initially decreases, followed by an increasing trend. Similar tendency was observed by Kayes et al. (2024). For instance, for the R1150/R744/R1234yf group, the consumption is 21.45 kW at −20 °C, decreases to 21.15 kW at −15 °C, and then starts to rise, reaching 23.05 kW at 5 °C.

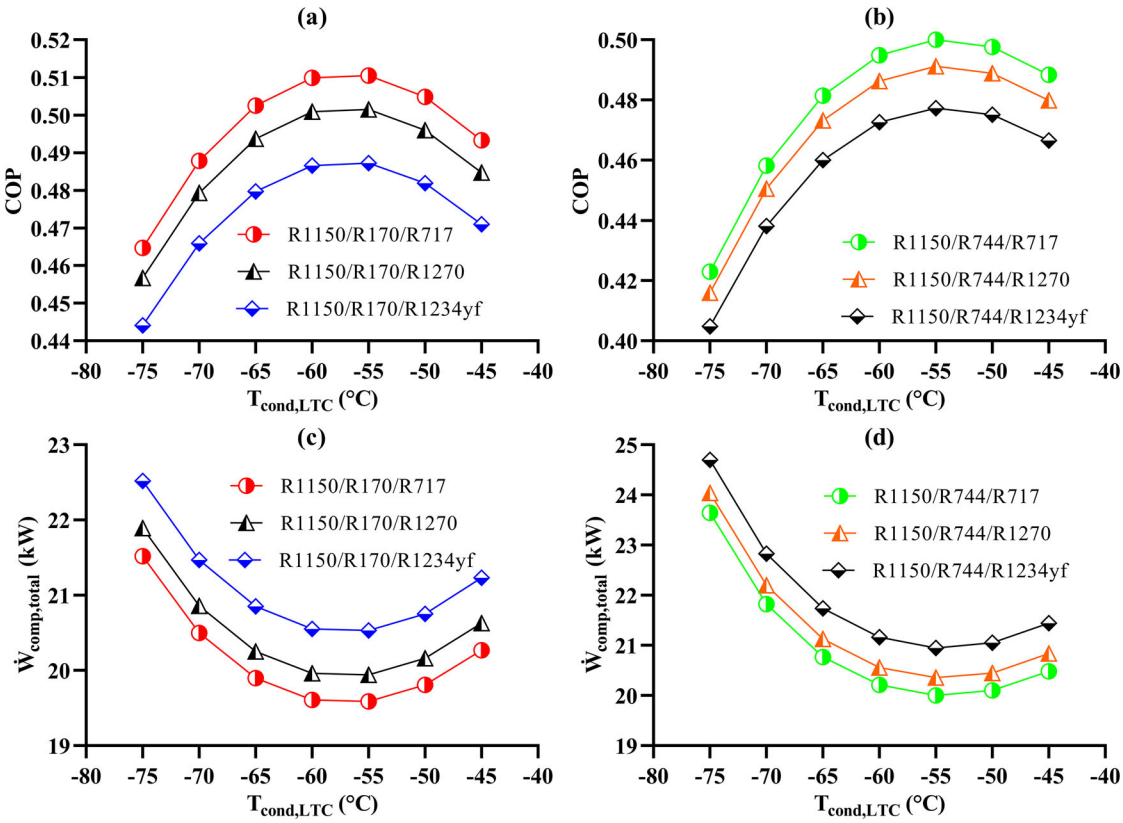

Fig. 6. Variation of COP and $\dot{W}_{comp,total}$ with $T_{cond,LTC}$.

Figure 9a,b show the effect of the variation in MTC condenser temperature on exergy efficiency for the six different refrigerant groups used. The results indicate that as $T_{cond,MTC}$ increases, exergy efficiency initially rises and then starts to decrease. For instance, for the R1150/R170/R1234yf group, the exergy efficiency is 0.32 at −20 °C, increases to 0.33 at −10 °C, and then follows a decreasing trend, reaching a minimum exergy efficiency of 0.3 at 5 °C.

Figure 9c,d present the change in the system's total exergy destruction as the MTC condenser temperature increases from −20 °C to 5 °C. The results show that as $T_{cond,MTC}$ increases, exergy destruction decreases up to a certain point, after which it starts to rise. For example, for the R1150/R744/R717 group, the exergy destruction is 13.44 kW at −20 °C, decreases to 13.3 kW at −15 °C, and then increases, reaching 15.76 kW at 5 °C. When comparing the refrigerants, it can be stated that the lowest exergy destruction occurs with the R1150/R170/R717 group across all analyzed $T_{cond,MTC}$ temperatures.

Figure 10a,b illustrate the change in COP as the HTC condenser temperature increases from 30 °C to 50 °C. The results show that as the condenser temperature rises, the COP decreases for all refrigerant groups. For example, for the R1150/R170/R1234yf group, the COP is 0.55 at a condenser temperature of 30 °C and decreases to 0.42 at 50 °C, resulting in a 23.6% reduction in COP. In their experimental study on the cascade refrigeration system, Cabello et al. (2023) reported that as the heat sink temperature of the condenser increases, and consequently the condenser temperature rises, a decrease in COP is observed. These results are consistent with the findings obtained in this study. In the experimental study on the cascade refrigeration system conducted by Zhang et al. (2020), it was found that an increase in the condenser temperature of the high-temperature cycle from 30 °C to 45 °C led to an 18.6% decrease in COP. In this study, a 20 °C increase in condenser temperature resulted in a 23.6% reduction in COP, indicating that the obtained results are consistent with the experimental studies in the literature.

Figure 10c,d show the effect of changes in the HTC condenser temperature on total compressor power consumption. The results indicate that as the condenser temperature increases, compressor consumption also increases. For instance, for the R1150/R744/R717 group, the compressor consumption is 18.27 kW at 30 °C and rises to 22.49 kW at 50 °C, resulting in a 23.1% increase in consumption. This increase in compressor consumption is reflected as a decrease in COP.

Figure 11a,b illustrate the effect of changes in the HTC condenser temperature on exergy efficiency. It is clear that as the condenser temperature increases, the system's exergy efficiency decreases. For example, for the R1150/R170/R1270 group, the exergy efficiency is 0.38 at 30 °C and decreases to 0.3 at 50 °C, resulting in a 21.1% reduction in exergy efficiency. The results indicate that across all the examined $T_{cond,HTC}$ temperature ranges, the R1150/R170/R717 group consistently exhibits the highest exergy efficiency.

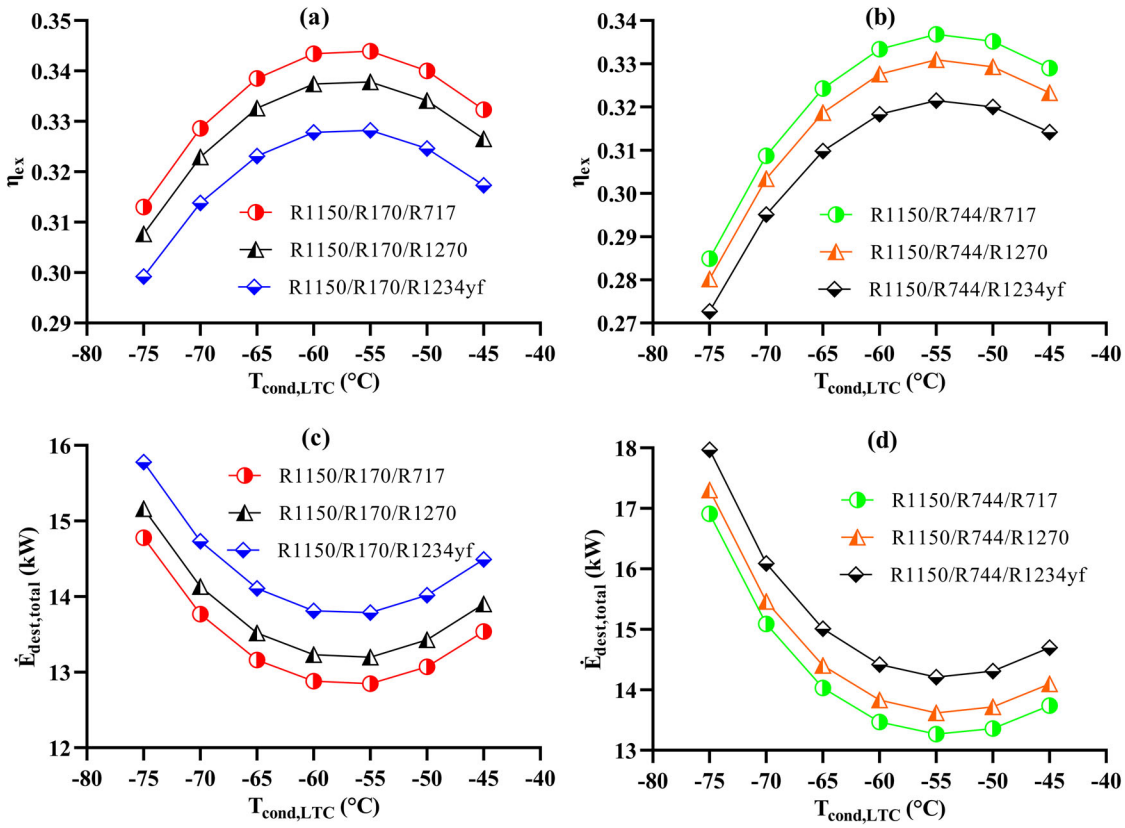

Fig. 7. Variation of η_{ex} and $\dot{E}_{dest,total}$ with $T_{cond,LTC}$.

Figure 11c,d show the change in the system's total exergy destruction as the HTC condenser temperature increases from 30 °C to 50 °C. The findings indicate that as $T_{cond,HTC}$ rises, exergy destruction increases. For example, for the R1150/R744/R1270 group, the exergy destruction is 11.68 kW at a condenser temperature of 30 °C and increases to 16.55 kW at 50 °C, resulting in a 41.7% increase in exergy destruction.

Figure 12a,b illustrate the change in COP as the temperature difference in the first cascade heat exchanger increases from 3 °C to 7 °C. The results indicate that an increase in the temperature difference in the cascade heat exchanger leads to a decrease in COP. For example, for the R1150/R170/R1234yf group, when the temperature difference in the cascade heat exchanger rises from 3 °C to 7 °C, the COP decreases from 0.5 to 0.47, resulting in a 6% reduction in COP.

Figure 12c,d illustrate the effect of an increase in the temperature difference in the first cascade heat exchanger on total compressor power consumption. The results show that an increase in the temperature difference in the cascade heat exchanger negatively impacts the system, leading to an increase in compressor power consumption. For example, for the R1150/R744/R1234yf refrigerant group, the rise in the temperature difference in the cascade heat exchanger from 3 °C to 7 °C causes the compressor consumption to increase from 20.43 kW to 21.96 kW, resulting in a 7.5% increase.

Figure 13a,b show the effect of changes in the temperature difference in the first cascade heat exchanger on exergy efficiency for all refrigerant groups. The results indicate that an increase in the temperature difference in the cascade heat exchanger leads to a decrease in the system's exergy efficiency. For example, in case of using the R1150/R170/R717 group, the exergy efficiency is 0.35 when the temperature difference in the cascade heat exchanger is 3 °C. However, as the temperature difference increases to 7 °C, the exergy efficiency decreases to 0.33, resulting in a 5.7% reduction in exergy efficiency.

Figure 13c,d present the findings regarding the change in total exergy destruction in the system as the temperature difference in the first cascade heat exchanger increases from 3 °C to 7 °C. The results indicate that an increase in the temperature difference in the cascade heat exchanger negatively impacts the system, leading to an increase in exergy destruction. For example, when using R1150/R744/R717, the exergy destruction is 12.76 kW with a 3 °C temperature difference in the cascade heat exchanger, and increases to 14.24 kW when the temperature difference rises to 7 °C, resulting in a 11.6% increase.

4.2. Machine learning results

MLP algorithm was selected due to its proven capability in capturing complex and non-linear relationships within datasets. MLP's multi-layer architecture allows it to model the interactions among features, which is advantageous for tasks where simple linear models may fall short. The dataset was standardized prior to model development. This

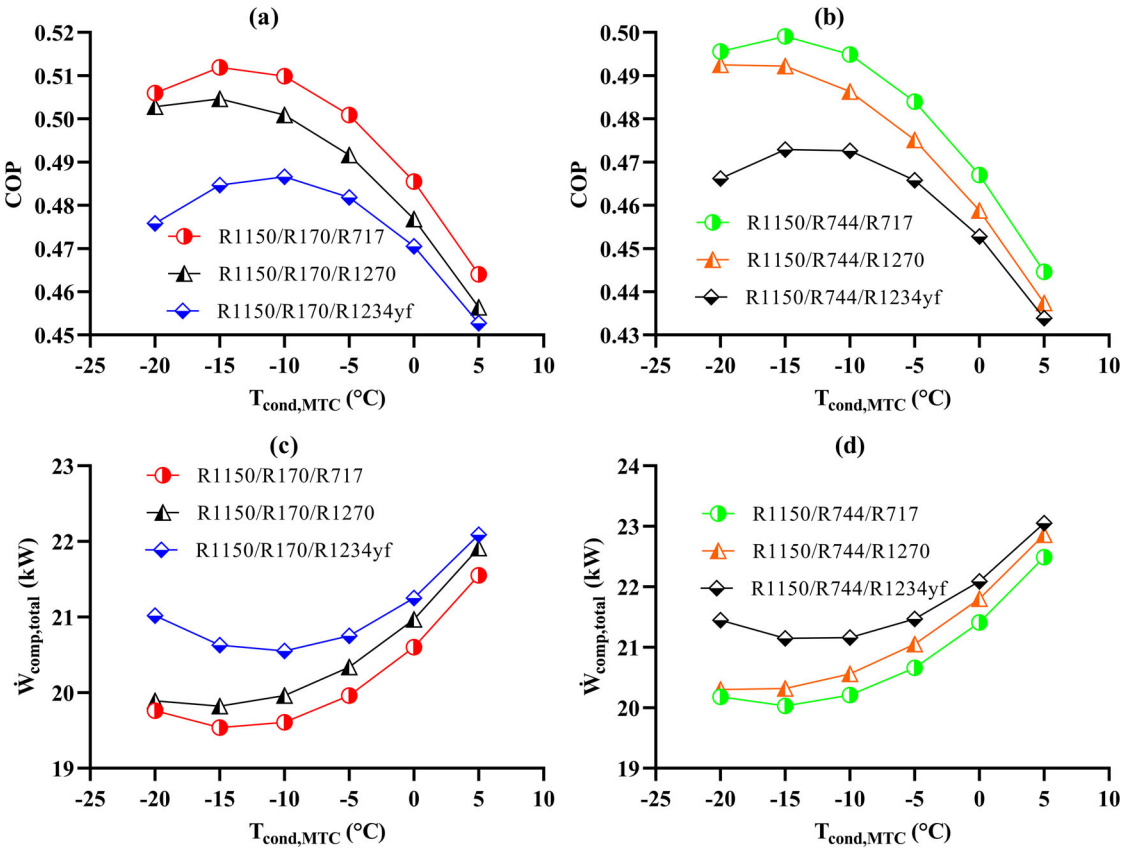

Fig. 8. Change of COP and $\dot{W}_{comp,total}$ with $T_{cond,MTC}$.

standardization process transforms the features to have a mean of zero and a standard deviation of one. By eliminating disparities in feature scales, the model's ability to learn and generalize is improved, preventing certain features from disproportionately influencing the training process. Overfitting prevention was achieved by splitting the dataset into training and testing subsets to evaluate generalization. Additionally, the optimal network architecture was identified, followed by fine-tuning of learning rate and momentum to minimize prediction errors without increasing model complexity. The 5-7-1-1 architecture, identified as the optimal network structure based on the performance evaluation of various MLP architectures, was used to determine the model with the minimum error by testing different learning rate and momentum values. It was found that the minimum error was achieved with a learning rate of 0.2 and a momentum of 0.3, completing the hyperparameter tuning process. The optimization of the MLP model was performed using the backpropagation algorithm. The activation function for the hidden layers was set to the sigmoid function. The sigmoid function was chosen as it effectively captures non-linear relationships in the data. The mean squared error loss function was applied since it is commonly used for regression tasks as it penalizes the difference between predicted and actual values, providing a smooth gradient for weight updates during training.

In MLP machine learning approach, evaporator temperature, LTC condenser temperature, MTC condenser temperature, HTC condenser temperature and the temperature difference of the number one cascade heat exchanger were used as inputs. In addition, COP, total compressor power consumption, total exergy destruction, and exergy efficiency were utilized as outputs in other words predicted parameters. Considering the results of the parametric analysis, the three most efficient points for the evaporator temperature are −95 °C, −90 °C, and −85 °C; for the LTC condenser temperature, they are −60 °C, −55 °C, and −50 °C; for the MTC condenser temperature, they are −20 °C, −15 °C, and −10 °C; for the HTC condenser temperature, they are 30 °C, 35 °C, and 40 °C; and for the first-stage cascade heat exchanger, they are 3 °C, 4 °C, and 5 °C. Therefore, a dataset for MLP predictions was created by considering all possible combinations of these points that lead to the highest efficiency. Additionally, this dataset was formed for the refrigerant group R1150/R170/R717, which was identified as the most efficient in the parametric analysis. The created dataset consists of a total of 1458 data points, with 70% of the data used to form the training set, resulting in 1020 data points in the training set. The remaining 30% of the data was used for the test set, which contains 438 data points. To ensure the reliability of the predictions, the data in the training and test sets were created in such a way that they do not overlap. The dataset was examined for duplicate entries, and any identified duplicates were removed to prevent bias during model training. Additionally, the dataset was checked for missing values, and no significant

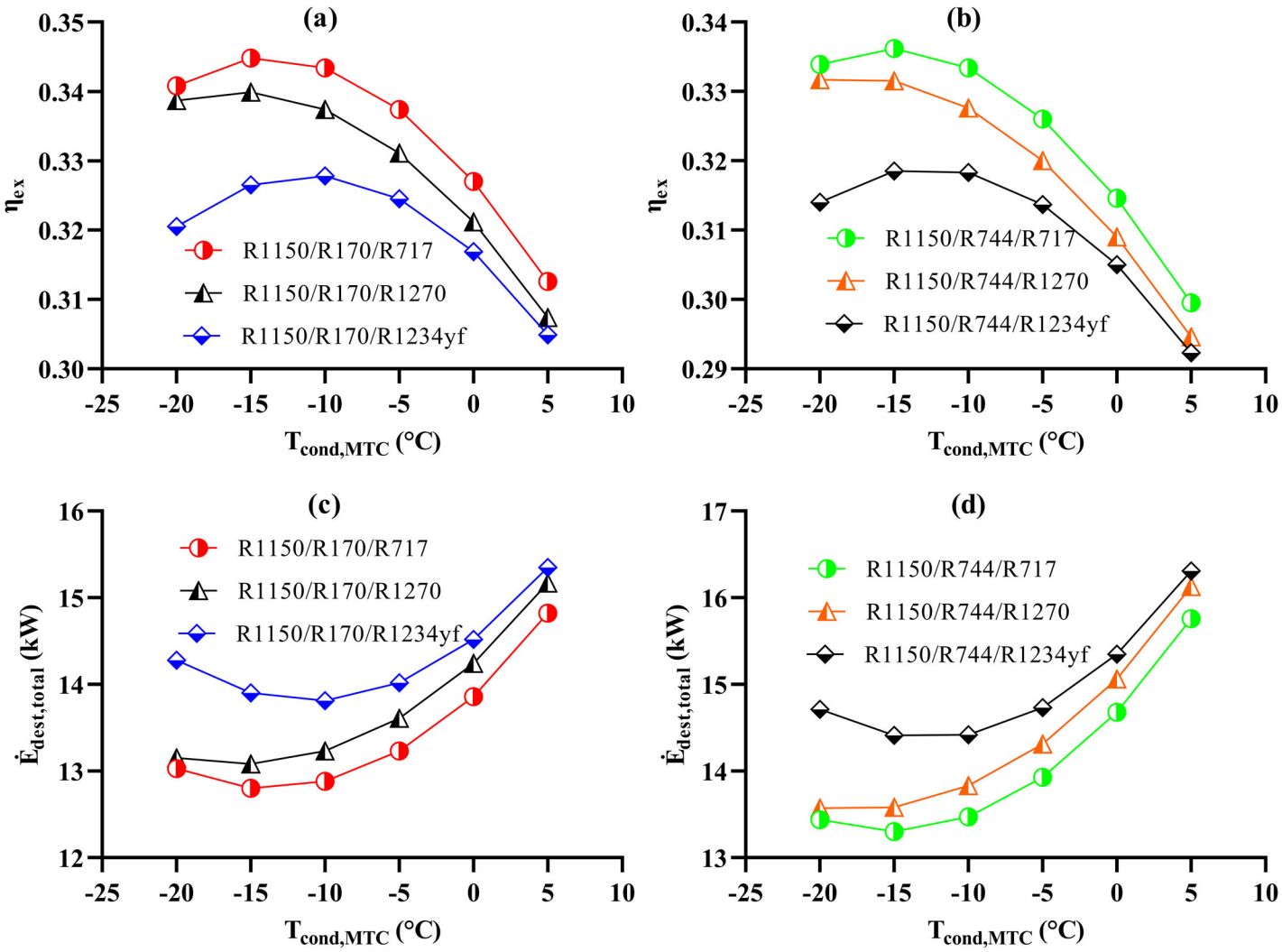

Fig. 9. Change of η_{ex} and $\dot{E}_{dest,total}$ with $T_{cond,MTC}$.

amount of missing data was detected. To prevent data overlap and maintain the integrity of the evaluation process, the data was randomly divided into training and testing subsets, ensuring that no same instances appeared in both sets. The prediction results were evaluated using the MAE and RMSE metrics, and the formulations of these metrics are shown in Equations 7 and 8. In MAE and RMSE equations, predicted value is represented by y, the real value is given with x, and n expresses the number of samples.

$$MAE = \frac{|y_1 - x_1| + \ldots + |y_n - x_n|}{n} \quad (7)$$

$$RMSE = \sqrt{\frac{1}{n}\sum_{i=1}^{n}(y_i - x_i)^2} \quad (8)$$

Figures 14 and 15 displays the prediction results for all parameters. In these figures, the pink circles represent the prediction results obtained using the MLP method, while the green diagonal line symbolizes the numerical results obtained from EES. In these graphs, the proximity of the pink circles to the green line indicates how closely the MLP method's predictions approach the EES numerical values, reflecting the accuracy of the predictions.

When examining the prediction results for COP and compressor power consumption in Figure 14, it is evident that the MLP method predicts both parameters with low error. For COP prediction, the MAE and RMSE in the training set are 0.0004 and 0.0006, respectively, while in the test set, they are 0.0006 and 0.0007. For compressor power consumption prediction, the training set results yield 0.0147 MAE and 0.0188 RMSE, while the test set results give 0.0193 MAE and 0.0268 RMSE.

In Figure 15, the prediction performance of the MLP method for exergy efficiency and total exergy destruction is shown, and considering the perfect alignment of the pink circles with the green line, it can be stated that both parameters are predicted with low error. For exergy efficiency prediction, the training set achieves 0.0002 MAE and 0.0003 RMSE, and when the model created with the training set is tested, it reaches 0.0003 MAE and 0.0003 RMSE. For total

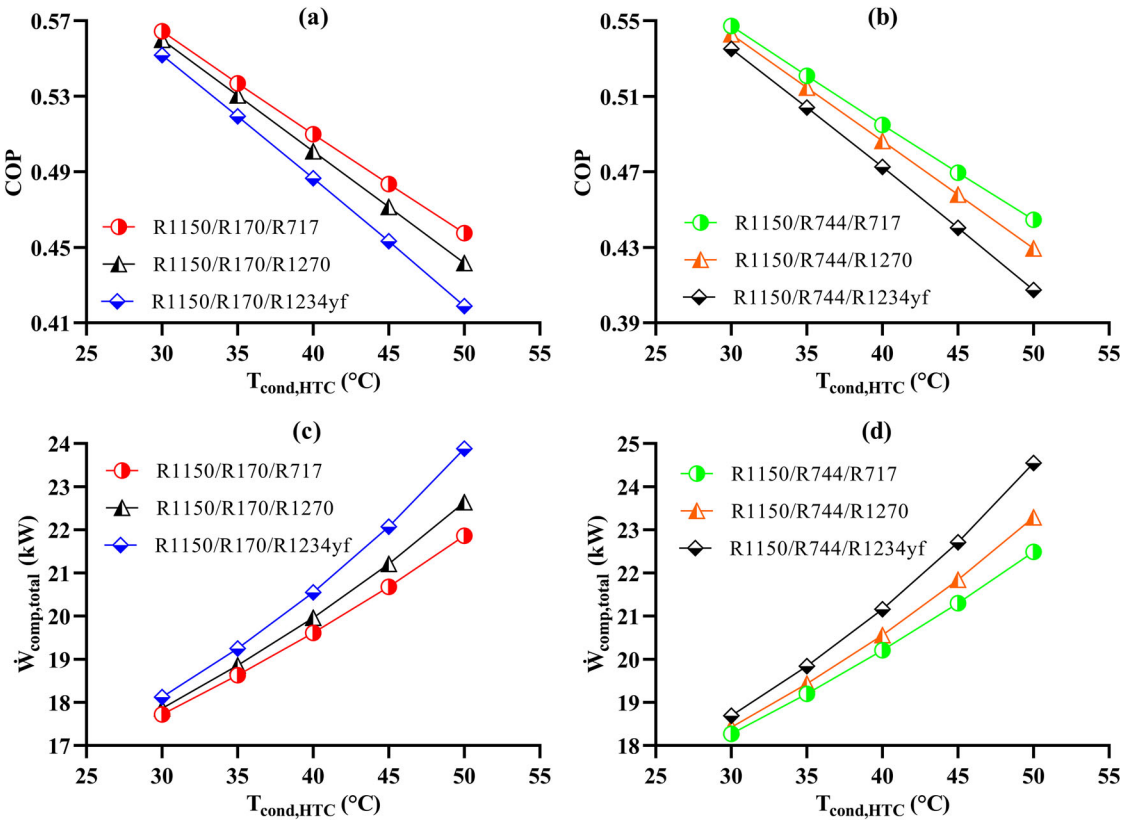

Fig. 10. Variation of COP and $\dot{W}_{comp,total}$ with $T_{cond,HTC}$.

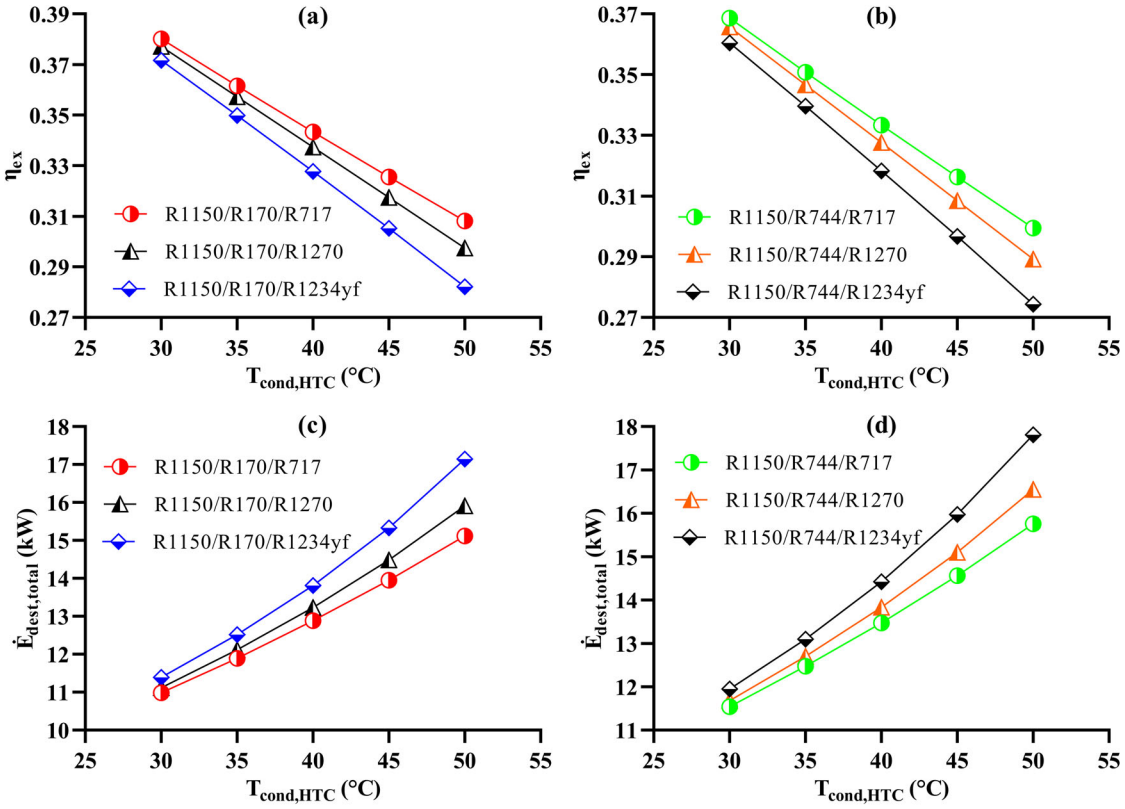

Fig. 11. Variation of η_{ex} and $\dot{E}_{dest,total}$ with $T_{cond,HTC}$.

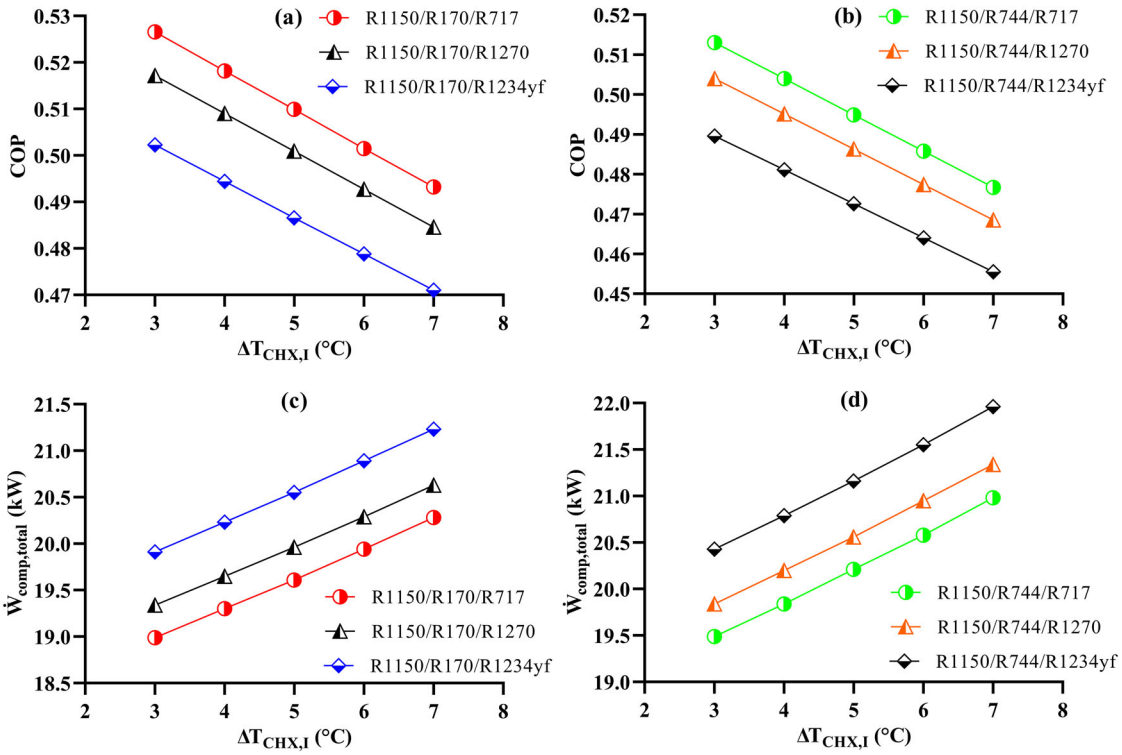

Fig. 12. Influence of $\Delta T_{CHX,I}$ on COP and $\dot{W}_{comp,total}$.

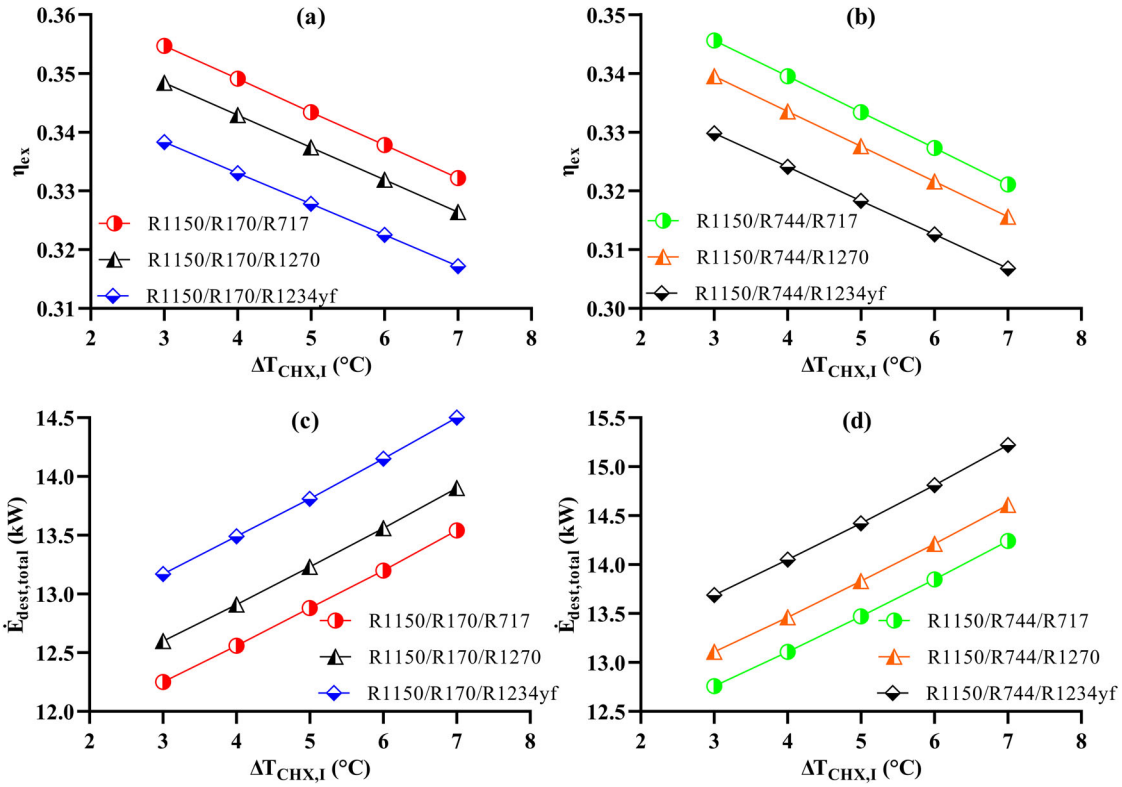

Fig. 13. Influence of $\Delta T_{CHX,I}$ on η_{ex} and $\dot{E}_{dest,total}$.

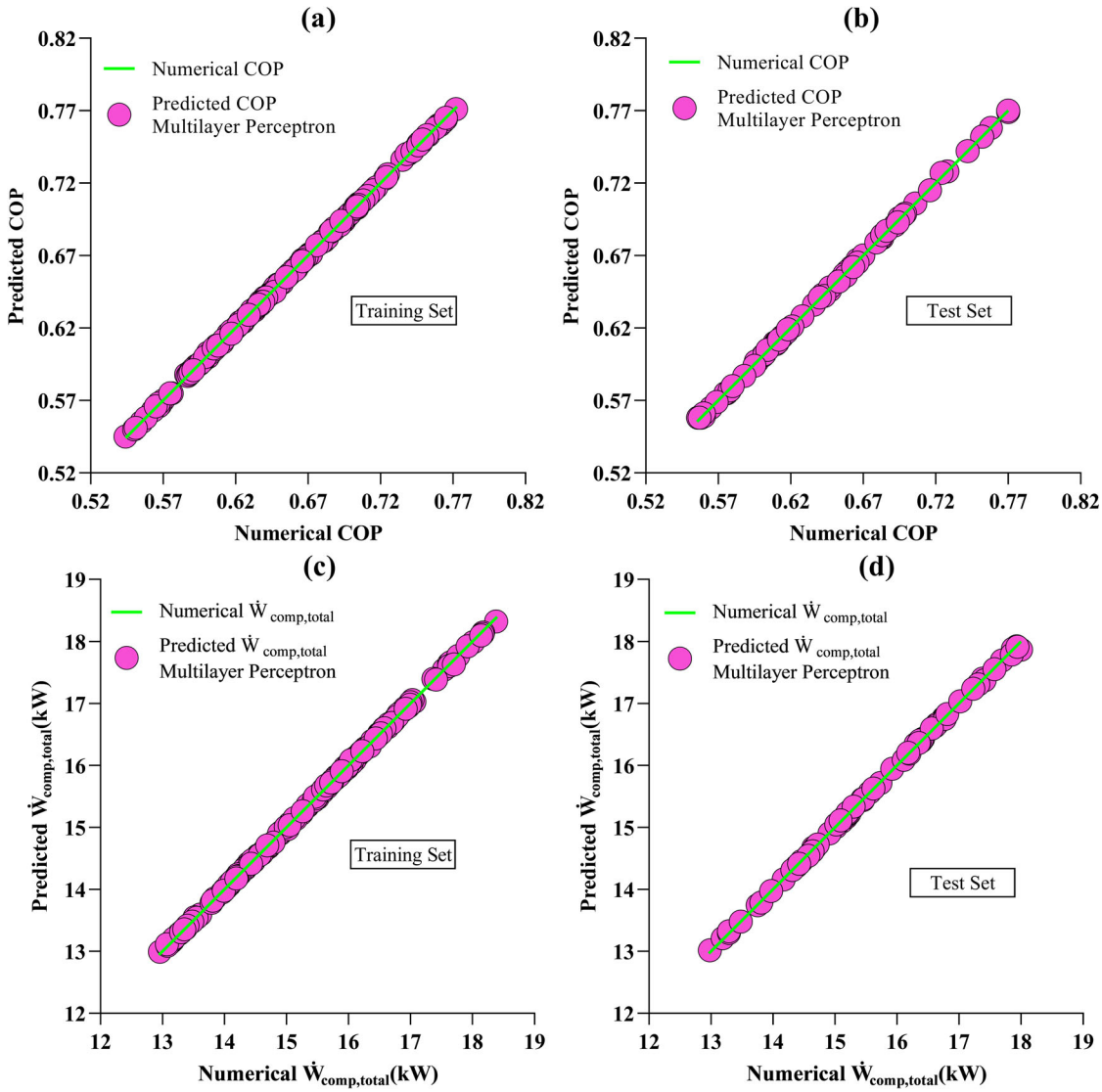

Fig. 14. COP and $\dot{W}_{comp,total}$ prediction results.

exergy destruction prediction, the MLP method yields 0.0178 MAE and 0.0214 RMSE in the training set, while in the test set, it reaches 0.0194 MAE and 0.0241 RMSE.

Figure 16 illustrates the prediction errors for COP, compressor consumption, exergy destruction, and exergy efficiency across the entire dataset. In these graphs, the error definitions on the y-axis show the difference between the values predicted using MLP and the corresponding EES numerical values. The zero point on the y-axis indicates the perfect prediction point. Large deviations from the zero point indicate poor predictions, while small deviations signify successful predictions. The x-axis represents the relevant data number related to the predicted value, covering both the training and test sets. Additionally, the prediction errors obtained using the MLP method are shown with red lines.

When examining the COP prediction errors shown in Figure 16a, it is observed that the MLP method results in a maximum error of 0.002 in the training set and 0.003 in the test set. Analyzing the error values for total compressor power consumption presented in Figure 16b, it can be seen that the maximum error in the training set is 0.071, while the maximum error in the test set is 0.132. The high prediction error of 0.132 observed in the specific data point (evaporator temperature of −95 °C, LTC condenser temperature of −60 °C, MTC condenser temperature of −10 °C, HTC condenser temperature of 40 °C, cascade heat exchanger temperature difference of 5 °C) in the test set of compressor power consumption model, can be attributed to the following factors: The model's ability to capture the full complexity of the input space may still be limited. In regions of the input space where data points are sparse or exhibit nonlinear interactions, the model may struggle to predict with high accuracy. This is reflected in slightly higher error rates in the test set compared to the training set. Addressing these discrepancies may require expanding the input range in the theoretical analysis. Although the dataset is representative of the operating conditions, certain regions, such as the one highlighted,

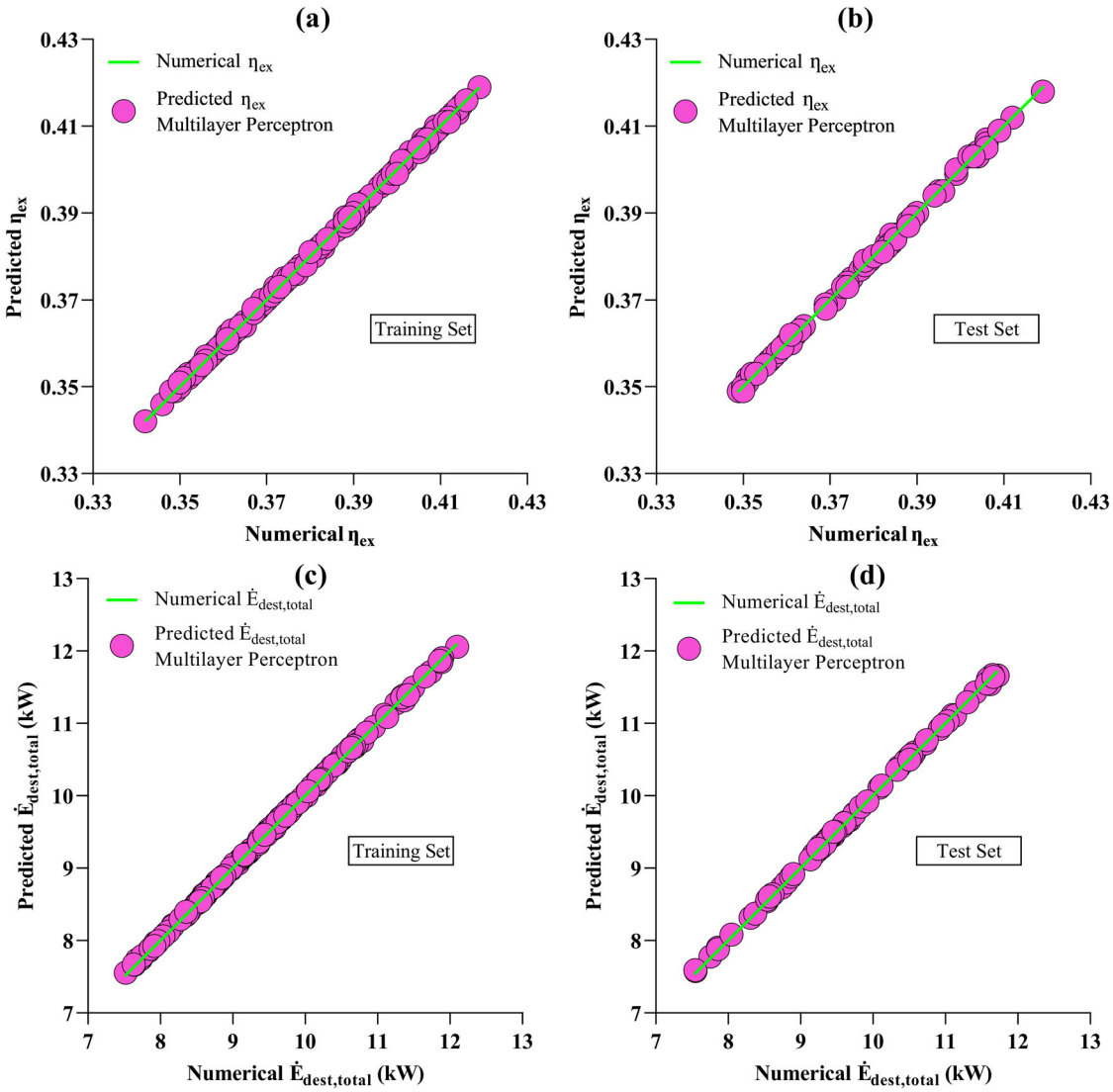

Fig. 15. η_{ex} and $\dot{E}_{dest,total}$ prediction results.

might be underrepresented during training. This can lead to slightly larger prediction errors when the model encounters less frequent or extreme scenarios. Overall, the test set performance remains within acceptable error margins, demonstrating good predictive capability across various operating conditions. Upon reviewing the findings in Figure 16c, which show the errors encountered in total exergy destruction prediction using the MLP approach, the maximum prediction error is 0.057 in the training set and 0.079 in the test set. For exergy efficiency, the prediction errors shown in Figure 16d indicate that the maximum error in both the training and test sets is 0.001. Overall, the findings in Figure 16 suggest that predictions for all parameters are made with high accuracy.

Figure 17 presents the cumulative frequency results for all predicted parameters. In Figure 17a, the COP cumulative frequency results indicate that 97% of the data are predicted with an absolute error of less than 0.002. Upon examining Figure 17b, it is observed that 95% of the data for total compressor power consumption are predicted with an absolute error of less than 0.04. Analyzing Figure 17c, it can be concluded that 98% of the data for total exergy destruction are predicted with an absolute error of less than 0.045. Finally, in Figure 17d, the exergy efficiency cumulative frequency results show that 75% of the data are predicted with an absolute error of less than 0.001.

Table 9 shows literature comparison of artificial intelligence studies used in cascade refrigeration systems. It is observed that the MLP models developed for the three-stage refrigeration cycle make predictions with lower errors for all parameters compared to the literature.

4.3. Economic analysis results

Economic analysis was performed for the R1150/R170/R717 refrigerant group to evaluate the costs associated with ultra-low temperature applications under an evaporator temperature of −105 °C, which enables achieving a very low room temperature of −100 °C.

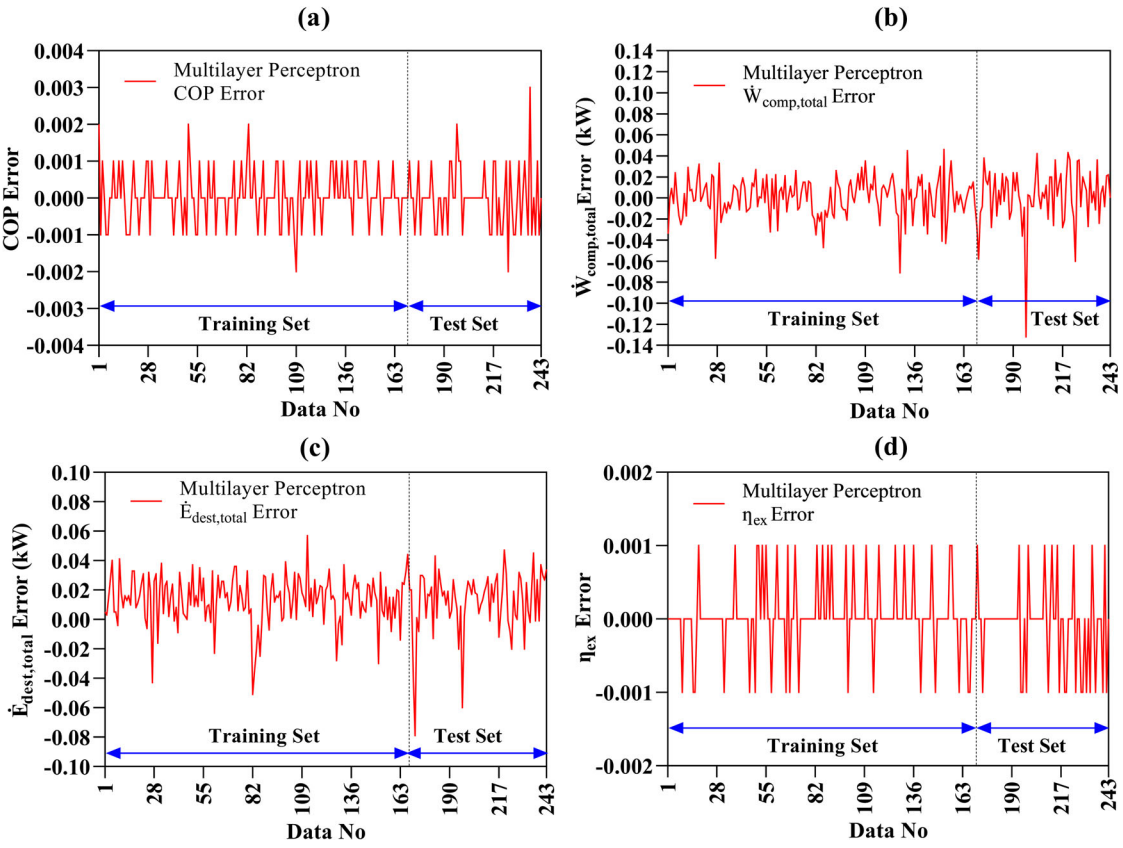

Fig. 16. COP, $\dot{W}_{comp,total}$, η_{ex} and $\dot{E}_{dest,total}$ prediction errors for entire data set.

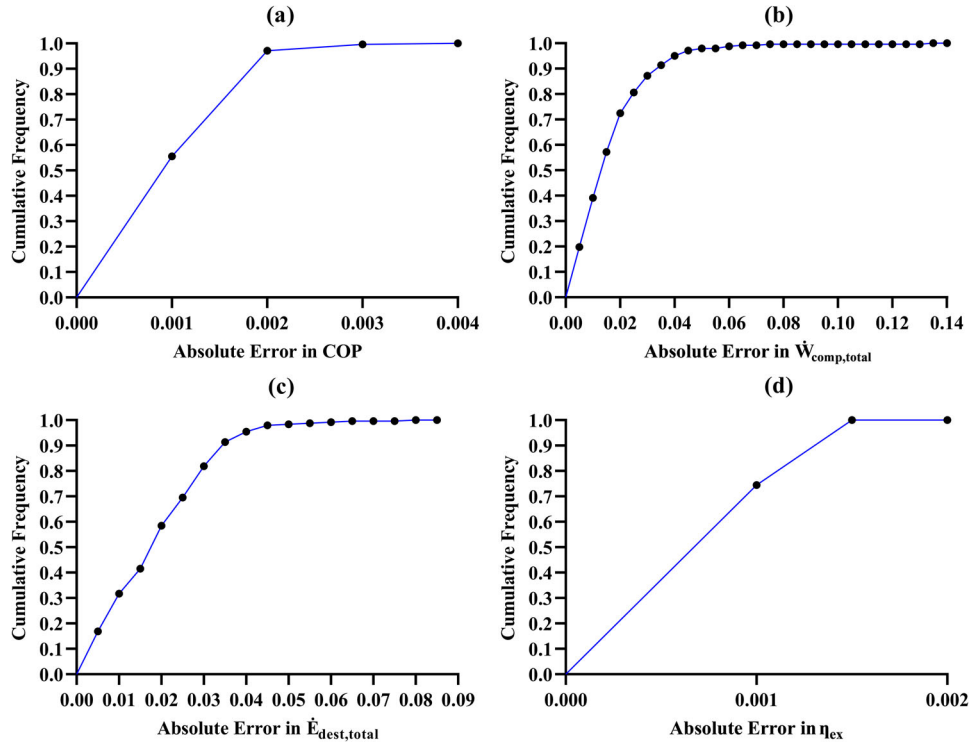

Fig. 17. Cumulative frequency of errors for COP, $\dot{W}_{comp,total}$, η_{ex} and $\dot{E}_{dest,total}$ predictions.

Table 9. Machine learning studies carried out in Cascade refrigeration systems.

Machine learning method	Evaluation metric	Notes	Reference
ANN	MAE: 0.0027, 0.9090, 0.1691, 1.0314	COP, $\dot{W}_{comp,total}$, η_{ex} and $\dot{E}_{dest,total}$ prediction in a two-stage cascade refrigeration configuration	(Ye et al. 2024b)
ANN	RMSE: 0.1	COP prediction in an experimental two-stage cascade refrigeration system	(Hosoz and Ertunc 2006)
GA-LSSVM (genetic algorithm- least square support vector machine)	RMSE: 3.3312, 3.3198	$\dot{W}_{comp,LTC}$ and $\dot{W}_{comp,HTC}$ prediction in a two-stage cascade refrigeration system	(Li et al. 2022)
MLP	MAE: 0.0006, 0.0193, 0.0003, and 0.0194 RMSE: 0.0007, 0.0268, 0.0003, 0.0241	COP, $\dot{W}_{comp,total}$, η_{ex} and $\dot{E}_{dest,total}$ prediction in a three-stage cascade refrigeration system	This study

Table 10. Cost functions for system components (Kayes et al. 2024).

Component	Cost function
HTC Compressor	$9624.2\dot{W}_{comp,HTC}^{0.46}$
HTC Expansion Valve	$114.5\cdot\dot{m}_{HTC}$
HTC Condenser	$1397\cdot A_{cond}^{0.89}$
Cascade Heat Exchanger II	$383.5\cdot A_{CHX,II}^{0.65}$
MTC Compressor	$9895.85\dot{W}_{comp,MTC}^{0.46}$
MTC Expansion Valve	$114.5\cdot\dot{m}_{MTC}$
Cascade Heat Exchanger I	$383.5\cdot A_{CHX,I}^{0.65}$
LTC Compressor	$10,167.5\dot{W}_{comp,LTC}^{0.46}$
LTC Expansion Valve	$114.5\cdot\dot{m}_{LTC}$
Evaporator	$1397\cdot A_{evap}^{0.89}$

The total cost of the entire system comprises capital and maintenance costs, penalty costs associated with CO_2 emissions, and operational costs. The system's whole cost can be calculated with Equation 9.

$$\dot{C}_{total}=\sum_{k}\dot{C}_k+\dot{C}_{env}+\dot{C}_{op} \quad (9)$$

Capital and maintenance costs ($\dot{C}_k$) are calculated with Equation 10. In this equation, C_k is the capital cost calculated depending on cost functions presented in Table 10. φ is maintenance factor and CRF is capital recovery factor.

$$\dot{C}_k=C_k\cdot\varphi\cdot CRF \quad (10)$$

CRF is calculated with Equation 11. In this equation, i represents the interest rate and n shows plant lifetime.

$$CRF=\frac{i(i+1)^n}{(i+1)^n-1} \quad (11)$$

Environmental penalty cost of the system ($\dot{C}_{env}$) is calculated with Equation 12. In this equation, m_{CO_2} is the mass of yearly discharged greenhouse gas and C_{CO_2} is the cost related with avoiding CO_2.

$$\dot{C}_{env}=m_{CO_2}\cdot C_{CO_2} \quad (12)$$

m_{CO_2} is calculated with Equation 13. In this equation, μ_{CO_2} is the emission factor and E_{annual} is the yearly electrical power consumption.

$$m_{CO_2}=\mu_{CO_2}\cdot E_{annual} \quad (13)$$

Operational costs ($\dot{C}_{op}$) are calculated with Equation 14. In this equation, N is the annual operation hour of the system, $\dot{W}_{total}$ is the total compressor consumption, and $\propto_{electricity}$ is the cost of electricity.

$$\dot{C}_{op}=N\cdot\dot{W}_{total}\cdot\propto_{electricity} \quad (14)$$

Estimating the costs of the heat exchangers in three stage cascade refrigeration system necessitates knowledge of their surface areas. To achieve this, Equation 15 is applied. In this equation, $\dot{Q}$ is the heat transfer rate, U is the overall heat transfer coefficient, and LMTD is logarithmic mean temperature difference.

$$A=\frac{Q}{U\cdot LMTD} \quad (15)$$

LMTD is calculated with Equation 16. In this equation, $T_{1,i}$ and $T_{1,o}$ are the inlet and outlet temperatures of hot flow while $T_{2,i}$ and $T_{2,o}$ are the inlet and outlet temperatures of cold flow.

$$LMTD=\frac{(T_{1,i}-T_{2,i})-(T_{1,o}-T_{2,o})}{\ln\frac{(T_{1,i}-T_{2,i})}{(T_{1,o}-T_{2,o})}} \quad (16)$$

Table 11 presents the results of economic analysis. When the results in Table 11 are examined, it is observed that the total cost of the plant is 43,379.8 $/year when the cooling room temperature of −100 °C is achieved.

Comparing the economic analysis results with previous studies in the literature, de Paula et al. (2021) calculated the

Table 11. Economic analysis findings of three stage cascade refrigeration system.

Parameter	Value
Capital and maintenance cost	29,061.3 $/year
CO_2 penalty cost	7042.84 $/year
Operational cost	7275.66 $/year
Total plant cost	43,379.8 $/year

total cost as 24,334 $/year for a two-stage cascade refrigeration system providing a cooling capacity of 10 kW and an evaporator temperature of −25 °C. The reason for the higher total plant cost in this study is the addition of an extra stage to achieve ultra-low temperatures like −100 °C, which are required for industrial cooling applications, thereby increasing costs. Achieving lower temperatures leads to an increase in compressor power consumption, thus raising costs. Here, since a two-stage cascade refrigeration system cannot reach the ultra-low temperatures required for industrial refrigeration, the additional costs brought by the three-stage configuration are inevitable. In another study conducted by Roy and Mandal (2020), the total plant cost was calculated as 57,254 $/year for a two-stage cascade refrigeration system providing a cooling capacity of 50 kW and an evaporator temperature of −33 °C. The cooling capacity in the mentioned study is higher than the 10 kW capacity selected in this study, which requires larger surface area heat exchangers, thereby increasing both capital and maintenance costs. Prajapati et al. (2024) calculated the total plant cost as 65,228 $/year for a two-stage cascade refrigeration system with a cooling capacity of 50 kW and an evaporator temperature of −25 °C. The difference in plant total costs is attributed to the higher cooling capacity selected in the mentioned study compared to the cooling capacity in this study. Sholahudin et al. (2016) determined the total plant cost as 49,341 $/year for a two-stage cascade refrigeration system providing a cooling capacity of 40 kW at an evaporator temperature of −50 °C. The total plant cost in the mentioned study is approximately 6000 $/year higher than the plant cost in this study.

This research contributes to the literature by delivering an extensive thermodynamic parametric evaluation of a three-stage cascade refrigeration system and constructing a precise MLP-based predictive model. This innovative methodology establishes a solid foundation for optimal design and performance prediction of ultra-low temperature refrigeration applications. Additionally, the economic analysis conducted for the three-stage cascade refrigeration system design will serve as a model for future experimental setups involving these systems.

5. Conclusions

In this study, the design of a three-stage cascade refrigeration system capable of achieving ultra-low temperatures has been developed. Initially, the performance of six refrigerant groups in the designed refrigeration system was examined under various conditions, and a parametric analysis was conducted. Following the parametric analysis, the most efficient refrigerant group and the operating conditions that provide the highest efficiency were determined. Based on this information, in the second part of the study, performance prediction was made using the MLP algorithm. Some notable findings from the study are listed below:

1. The findings show that an increase in the evaporator temperature leads to an improvement in both COP and exergy efficiency, while reducing compressor consumption and exergy destruction. As the LTC condenser temperature and MTC condenser temperature increase, COP and exergy efficiency initially rise, but then begin to decrease. On the other hand, an increase in the HTC condenser temperature and the temperature difference in the cascade heat exchanger negatively affects the system, causing a decline in both COP and exergy efficiency.
2. As a result of the parametric analysis, the R1150/R170/R717 refrigerant group emerged as the most efficient working fluid combination. With this refrigerant group, under the conditions of an −85 °C evaporator temperature, −60 °C LTC condenser temperature, -10 °C MTC condenser temperature, 40 °C HTC condenser temperature, and a 5 °C temperature difference in the cascade heat exchanger, a COP of 0.65 and an exergy efficiency of 0.35 were achieved.
3. The economic analysis results carried out to achieve a cooling room temperature of -100 °C and cooling capacity of 10 kW indicate that the total plant cost is 43,379.8 $/year.
4. The prediction results obtained using MLP show that predictions were made with low errors for all parameters. For the predictions of COP, total compressor power consumption, exergy efficiency, and total exergy destruction, the MAE values obtained for the test set were 0.0006, 0.0193, 0.0003, and 0.0194, respectively. This study indicates that MLP is successful for prediction, system design, and performance optimization in ultra-low temperature refrigeration systems.

The increasing demand for refrigeration systems operating at ultra-low temperatures, especially due to Covid-19, led to the design of a three-stage cascade refrigeration system in this study. Significant results regarding the potential use of the environmentally friendly R1150/R170/R717 refrigerant group in three-stage cascade refrigeration systems have been obtained. The great agreement between the numerical EES findings and the MLP predictions indicates the fact that machine learning can successfully model the three-stage cascade refrigeration system's thermal behavior. It is clear that the findings from this study will benefit companies designing cabinets for ultra-low temperature operations and relevant researchers. For future studies, the establishment of an experimental setup for the three-stage cascade refrigeration system and the application of different artificial intelligence methods to this system are planned. Models enhanced by larger data sets and experimental measurement data developed for this purpose will contribute to the establishment of smarter, more efficient, and environmentally sustainable

refrigeration systems in the future. In addition, the implementation of environmental and economic analyses could help in the more comprehensive evaluation of these systems.

Disclosure statement

No potential conflict of interest was reported by the author(s).

Notes on contributor

Oguzhan Pektezel, BSc, MSc, PhD, is an Assistant Professor.

References

Abas, N., A. R. Kalair, N. Khan, A. Haider, Z. Saleem, and M. S. Saleem. 2018. Natural and synthetic refrigerants, global warming: A review. *Renewable and Sustainable Energy Reviews* 90:557–69. doi:10.1016/j.rser.2018.03.099

Afzal, S., B. M. Ziapour, A. Shokri, H. Shakibi, and B. Sobhani. 2023. Building energy consumption prediction using multilayer perceptron neural network-assisted models; comparison of different optimization algorithms. *Energy* 282:128446. doi:10.1016/j.energy.2023.128446

Alsouda, F., N. S. Bennett, S. C. Saha, F. Salehi, and M. S. Islam. 2023. Vapor compression cycle: A state-of-the-art review on cycle improvements, water and other natural refrigerants. *Clean Technologies* 5 (2):584–608. doi:10.3390/cleantechnol5020030

Bingming, W., W. Huagen, L. Jianfeng, and X. Ziwen. 2009. Experimental investigation on the performance of NH_3/CO_2 cascade refrigeration system with twin-screw compressor. *International Journal of Refrigeration* 32 (6):1358–65. doi:10.1016/j.ijrefrig.2009.03.008

Cabello, R., A. Andreu-Nácher, D. Sánchez, R. Llopis, and F. Vidan-Falomir. 2023. Energy comparison based on experimental results of a cascade refrigeration system pairing R744 with R134a, R1234ze (E) and the natural refrigerants R290, R1270, R600a. *International Journal of Refrigeration* 148:131–42. doi:10.1016/j.ijrefrig.2023.01.009

Chen, M., Q. Yang, B. Shi, X. Chen, W. Chi, G. Liu, Y. Zhao, and L. Li. 2023. Performance comparison of ultra-low temperature cascade refrigeration cycles using R717/R170, R717/R41 and R717/R1150 to replace R404A/R23. *Thermal Science and Engineering Progress* 44:102048. doi: doi:10.1016/j.tsep.2023.102048.

Das, M., and O. Pektezel. 2022. Experimental and numerical comparison of thermodynamic performances of new and old generation refrigerants in the same cooling system. *Thermal Science* 26 (6):4841–54. doi:10.2298/TSCI220205069D

Das, M., O. Pektezel, and E. Alic. 2022. Experimental and numerical investigation of thermal performances of R290 and R1234yf refrigerants in a cold room. *Science and Technology for the Built Environment* 28 (8):970–84. doi:10.1080/23744731.2022.2085474

de Paula, C. H., W. M. Duarte, T. T. M. Rocha, R. N. de Oliveira, and A. A. T. Maia. 2021. Energetic, exergetic, environmental, and economic assessment of a cascade refrigeration system operating with four different ecological refrigerant pairs. *International Journal of Air-Conditioning and Refrigeration* 29 (03):2150025. doi:10.1142/S2010132521500255

Dopazo, J. A., and J. Fernández-Seara. 2011. Experimental evaluation of a cascade refrigeration system prototype with CO_2 and NH_3 for freezing process applications. *International Journal of Refrigeration* 34 (1):257–67. doi:10.1016/j.ijrefrig.2010.07.010

Faruque, M. W., M. R. Uddin, S. Salehin, and M. Monjurul Ehsan. 2022. A Comprehensive Thermodynamic Assessment of Cascade Refrigeration System Utilizing Low GWP Hydrocarbon Refrigerants. *International Journal of Thermofluids* 15:100177. doi: doi:10.1016/j.ijft.2022.100177.

Faruque, Md, W., M. H. Nabil, M. R. Uddin, M. Monjurul Ehsan, and S. Salehin. 2022. Thermodynamic assessment of a triple cascade refrigeration system utilizing hydrocarbon refrigerants for ultra-low temperature applications. *Energy Conversion and Management* 14:100207. doi: doi:10.1016/j.ecmx.2022.100207.

Gullo, P., B. Elmegaard, and G. Cortella. 2016. Advanced exergy analysis of a R744 booster refrigeration system with parallel compression. *Energy* 107:562–71. doi:10.1016/j.energy.2016.04.043

Hamzaoui, M., A. Hadiouche, and S. Tiachacht. 2024a. Enhancing energy, exergy, and environment performances of ultra-low-temperature three-stage cascade refrigeration cycle: optimization and comparative analysis. *Arabian Journal for Science and Engineering*:1–29. doi:10.1007/s13369-024-09817-6

Hamzaoui, M., S. Tiachacht, and A. Hadiouche. 2024b. Optimization of a three-stage cascade refrigeration system operating with natural refrigerants to produce low temperatures by applying a bio-inspired method. *Thermal Science and Engineering Progress* 50:102519. doi: doi:10.1016/j.tsep.2024.102519.

Harby, K. 2017. Hydrocarbons and their mixtures as alternatives to environmental unfriendly halogenated refrigerants: An updated overview. *Renewable and Sustainable Energy Reviews* 73:1247–64. doi:10.1016/j.rser.2017.02.039

Hosoz, M., and H. M. Ertunc. 2006. Modelling of a cascade refrigeration system using artificial neural network. *International Journal of Energy Research* 30 (14):1200–15. doi:10.1002/er.1218

Jeon, M.-J. 2021. Experimental analysis of the R744/R404A cascade refrigeration system with internal heat exchanger. Part 1: Coefficient of performance characteristics. *Energies* 14 (18):6003. doi:10.3390/en14186003

Ji, S., Z. Liu, H. Pan, and X. Li. 2024. Energy, exergy, environmental and exergoeconomic (4E) analysis of an ultra-low temperature cascade refrigeration system with environmental-friendly refrigerants. *Applied Thermal Engineering* 248:123210. doi: doi:10.1016/j.applthermaleng.2024.123210.

Jin, H., Y.-G. Kim, Z. Jin, A. A. Rushchitc, and A. S. Al-Shati. 2022. Optimization and analysis of bioenergy production using machine learning modeling: Multi-layer perceptron, Gaussian processes regression, K-nearest neighbors, and Artificial neural network models. *Energy Reports* 8:13979–96. doi:10.1016/j.egyr.2022.10.334

Kayes, I., R. E. Ratul, A. Abid, F. B. Majmader, Y. Khan, and M. M. Ehsan. 2024. Multi-objective optimization and 4E (energy, exergy, economy, environmental impact) analysis of a triple cascade refrigeration system. *Heliyon* 10 (11):e31655. doi: doi:10.1016/j.heliyon.2024.e31655.

Klein, S. A. 2013. *Engineering equation solver (EES)*. Middleton: Academic Professional Version F-Chart Software.

Li, Y., X. Pan, X. Liao, and Z. Xing. 2022. A data-driven energy management strategy based on performance prediction for cascade refrigeration systems. *International Journal of Refrigeration* 136:114–23. doi:10.1016/j.ijrefrig.2022.01.012

Liu, R., D. Bacellar, and V. Aute. 2023. Review of systems and refrigerants for ultra-low temperature refrigeration. ASHRAE Transactions 129. doi:10.63044/w23liu23

Mosavi, A., M. Salimi, S. Faizollahzadeh Ardabili, T. Rabczuk, S. Shamshirband, and A. R. Varkonyi-Koczy. 2019. State of the art of machine learning models in energy systems, a systematic review. *Energies* 12 (7):1301. doi:10.3390/en12071301

Mota-Babiloni, A., P. Makhnatch, and R. Khodabandeh. 2017. Recent investigations in HFCs substitution with lower GWP synthetic alternatives: Focus on energetic performance and environmental impact. *International Journal of Refrigeration* 82:288–301. doi:10.1016/j.ijrefrig.2017.06.026

Mota-Babiloni, A., M. Mastani Joybari, J. Navarro-Esbrí, C. Mateu-Royo, Á. Barragán-Cervera, M. Amat-Albuixech, and F. Molés. 2020. Ultralow-temperature refrigeration systems: Configurations and refrigerants to reduce the environmental impact. *International Journal of Refrigeration* 111:147–58. doi: doi:10.1016/j.ijrefrig.2019.11.016.

Nabil, M. H., Y. Khan, M. W. Faruque, and M. M. Ehsan. 2023. Thermo-economic assessment of advanced triple cascade refrigeration system incorporating a flash tank and suction line heat exchanger. *Energy Conversion and Management* 295:117630. doi:10.1016/j.enconman.2023.117630

Orrù, P. F., A. Zoccheddu, L. Sassu, C. Mattia, R. Cozza, and S. Arena. 2020. Machine learning approach using MLP and SVM algorithms for the fault prediction of a centrifugal pump in the oil and gas industry. *Sustainability* 12 (11):4776. doi:10.3390/su12114776

Pektezel, O., M. Das, and H. I. Acar. 2023a. Experimental exergy analysis of low-GWP R290 refrigerant and derivation of exergetic performance equations with regression algorithms. *International Journal of Exergy* 40 (4):467–82. doi:10.1504/IJEX.2023.130371

Pektezel, O., M. Das, and H. I. Acar. 2023b. Experimental analysis of different refrigerants' thermal behavior and predicting their performance parameters. *Journal of Thermophysics and Heat Transfer* 37 (2):309–19. doi:10.2514/1.T6660

Prajapati, P., V. Patel, B. D. Raja, and H. Jouhara. 2024. Energy-exergy-economic-environmental (4E) analysis and multi-objective optimization of a cascade refrigeration system. *Thermal Science and Engineering Progress* 54:102793. doi:10.1016/j.tsep.2024.102793

Rezayan, O., and A. Behbahaninia. 2011. Thermoeconomic optimization and exergy analysis of CO2/NH3 cascade refrigeration systems. *Energy* 36 (2):888–95. doi:10.1016/j.energy.2010.12.022

Rogala, Z., and A. Kwiatkowski. 2022. Modeling of a three-stage cascaded refrigeration system based on standard refrigeration compressors in cryogenic applications above 110 K. *Modelling* 3 (2):255–71. doi:10.3390/modelling3020017

Roy, R., and B. K. Mandal. 2019. Energetic and exergetic performance comparison of cascade refrigeration system using R170-R161 and R41-R404A as refrigerant pairs. *Heat and Mass Transfer* 55 (3):723–31. doi: doi:10.1007/s00231-018-2455-7.

Roy, R., and B. K. Mandal. 2020. Thermo-economic analysis and multi-objective optimization of vapour cascade refrigeration system using different refrigerant combinations: A comparative study. *Journal of Thermal Analysis and Calorimetry* 139:3247–61.

Sholahudin, S., N. Giannetti, Nasruddin, and Arnas, 2016. Optimization of a cascade refrigeration system using refrigerant C_3H_8 in high temperature circuits (HTC) and a mixture of C_2H_6/CO_2 in low temperature circuits (LTC). *Applied Thermal Engineering* 104:96–103. doi:10.1016/j.applthermaleng.2016.05.059

Sanz-Kock, C., R. Llopis, D. Sánchez, R. Cabello, and E. Torrella. 2014. Experimental evaluation of a R134a/CO_2 cascade refrigeration plant. *Applied Thermal Engineering* 73 (1):41–50. doi:10.1016/j.applthermaleng.2014.07.041

Singha, P., M. Sankar Dasgupta, S. Bhattacharyya, and A. Hafner. 2024. Energy, environmental, and economic analysis of novel R744/R290 cascade refrigeration systems designed for warm ambient conditions utilizing ejector. *Thermal Science and Engineering Progress* 53:102724. doi:10.1016/j.tsep.2024.102724

Sumardi, K., N. Nahadi, and M. Mutaufiq. 2020. Experimental study of hydrocarbon refrigerant (R-1270) to replace R-32 in residential air conditioning system. *Journal of Physics: Conference Series* 1469 (1):012174. doi:10.1088/1742-6596/1469/1/012174

Sun, Z., Y. Liang, S. Liu, W. Ji, R. Zang, R. Liang, and Z. Guo. 2016. Comparative analysis of thermodynamic performance of a cascade refrigeration system for refrigerant couples R41/R404A and R23/R404A. *Applied Energy* 184:19–25. doi: doi:10.1016/j.apenergy.2016.10.014.

Sun, Z., and Y. Wang. 2022. Comprehensive performance analysis of cascade refrigeration system with two-stage compression for industrial refrigeration. *Case Studies in Thermal Engineering* 39:102400. doi: doi:10.1016/j.csite.2022.102400.

Sun, Z., Q. Wang, B. Dai, M. Wang, and Z. Xie. 2019a. Options of low Global Warming Potential refrigerant group for a three-stage cascade refrigeration system. *International Journal of Refrigeration* 100:471–83. doi: doi:10.1016/j.ijrefrig.2018.12.019.

Sun, Z., Q. Wang, Z. Xie, S. Liu, D. Su, and Q. Cui. 2019b. Energy and exergy analysis of low GWP refrigerants in cascade refrigeration system. *Energy* 170:1170–80. doi: doi:10.1016/j.energy.2018.12.055.

Tatar, A. B. 2025. Predicting three-dimensional (3D) printing product quality with machine learning-based regression methods. *Firat University Journal of Experimental and Computational Engineering* 4 (1):206–25. doi:10.62520/fujece.1604379

Uddin, K., and B. B. Saha. 2022. An overview of environment-friendly refrigerants for domestic air conditioning applications. *Energies* 15 (21):8082. doi:10.3390/en15218082

Udroiu, C.-M., A. Mota-Babiloni, and J. Navarro-Esbrí. 2022. Advanced two-stage cascade configurations for energy-efficient -80 degrees C refrigeration. *Energy Conversion and Management* 267:115907. doi: doi:10.1016/j.enconman.2022.115907.

Ustaoglu, A., B. Kursuncu, M. Alptekin, and M. Sabri Gok. 2020. Performance optimization and parametric evaluation of the cascade vapor compression refrigeration cycle using Taguchi and ANOVA methods. *Applied Thermal Engineering* 180:115816. doi: doi:10.1016/j.applthermaleng.2020.115816.

Vuppaladadiyam, A. K., E. Antunes, S. S. V. Vuppaladadiyam, Z. T. Baig, A. Subiantoro, G. Lei, S.-Y. Leu, A. K. Sarmah, and H. Duan. 2022. Progress in the development and use of refrigerants and unintended environmental consequences. *The Science of the Total Environment* 823:153670. doi:10.1016/j.scitotenv.2022.153670

Ye, W., F. Liu, Y. Yan, and Y. Liu. 2024a. Application of response surface methodology and desirability approach to optimize the performance of an ultra-low temperature cascade refrigeration system. *Applied Thermal Engineering* 239:122130. doi: doi:10.1016/j.applthermaleng.2023.122130.

Ye, W., Y. Yan, Z. Zhou, and P. Yang. 2024b. Parametric analysis and performance prediction of an ultra-low temperature cascade refrigeration freezer based on an artificial neural network. *Case Studies in Thermal Engineering* 55:104162. doi: doi:10.1016/j.csite.2024.104162.

Zhang, Z., G. He, Q. Hou, Y. Zou, J. Hua, W. Yang, and Z. Wang. 2024. Experimental and mechanism study on the flammability of the mixtures of propylene and ethane. *Fuel* 360:130590. doi:10.1016/j.fuel.2023.130590

Zhang, Z., G. He, Q. Ning, Z. Wang, W. Yang, J. Hua, and S. Zhou. 2023. Evaluation of flammability characteristics of mixed refrigerants R134a/R1270, R134a/R170, and R170/R1270. *International Journal of Refrigeration* 156:1–11. doi:10.1016/j.ijrefrig.2023.09.013

Zhang, Y., Y. He, Y. Wang, X. Wu, M. Jia, and Y. Gong. 2020. Experimental investigation of the performance of an R1270/CO_2 cascade refrigerant system. *International Journal of Refrigeration* 114:175–80. doi:10.1016/j.ijrefrig.2020.02.017